KATHOLIEKE UNIVERSITEIT LEUVEN
FACULTEIT GENEESKUNDE
BIOMEDISCHE WETENSCHAPPEN

Effect van intralesionale elektrische stimulatie op hippocampale ritmes in een acuut model van een mediaal septaal microletsel

(Effects of intralesional electrical stimulation on hippocampal rhythms in an acute model of a medial septal microlesion)

Masterproef voorgedragen
tot het behalen van de
graad van Master in de
Biomedische Wetenschappen
door Katrien MOLS

Promotor: Prof. dr. Bart NUTTIN
Faculteit Geneeskunde
Departement Neurowetenschappen
Afdeling Experimentele Neurochirurgie en Neuro-anatomie
Laboratorium voor Experimentele Functionele Neurochirurgie

Begeleider: Dr. Dimiter PRODANOV, MD PhD
IMEC (SSET)
Departement BIONE
Bioelectronic Systems group

Leuven, 2011

KATHOLIEKE UNIVERSITEIT LEUVEN
FACULTEIT GENEESKUNDE
BIOMEDISCHE WETENSCHAPPEN

Effect van intralesionale elektrische stimulatie op hippocampale ritmes in een acuut model van een mediaal septaal microletsel

(Effects of intralesional electrical stimulation on hippocampal rhythms in an acute model of a medial septal microlesion)

Masterproef voorgedragen
tot het behalen van de
graad van Master in de
Biomedische Wetenschappen
door Katrien MOLS

Promotor: Prof. dr. Bart NUTTIN
Faculteit Geneeskunde
Departement Neurowetenschappen
Afdeling Experimentele Neurochirurgie en Neuro-anatomie
Laboratorium voor Experimentele Functionele Neurochirurgie

Begeleider: Dr. Dimiter PRODANOV, MD PhD
IMEC (SSET)
Departement BIONE
Bioelectronic Systems group

Leuven, 2011

Acknowledgements

Making a master thesis is not an easy task, but it would have been impossible without the help and support from numerous people. Therefore, I would first like to express my gratitude to my promoter, professor Nuttin, who enabled me to start this project and guided me through it with wise advice. I wish to thank my supervisor at IMEC, Dimiter, who undertook the difficult task of introducing me to the world of electrophysiology and convincing me there are no default settings in it. I greatly appreciate Ivan for running complex analyses on my data and providing me with more insight into them. Many thanks also to the people from the Laboratorium voor Experimentele Functionele Neurochirurgie en IMEC, Kris, Marleen, Laura, Hemmings and Seon-Ah for their trainings, their indispensable suggestions and support. Of course a thanks to Olga, who was always prepared to help me out and assisted me with the 'Nissl mass production line'. Furthermore, I would like to say 'thank you' to my family who made sure I received the mental support when I needed it throughout the trials and tribulations of this thesis and especially to my sister Liesbet for her artwork and my sister Laurien for assisting me at the finish. On a special note, I would finally like to thank Kristina, who went through the same process and who I could always rely on.

Summary

The medial septum (MS) is tightly connected with the hippocampus (HC). Electrolytic MS lesions can decrease theta rhythm (3-12 Hz) in the dorsal hippocampus, while electrical stimulation in the theta range in this area is capable of evoking a HC rhythm with the same frequency. The aim of the present experiment was to establish whether electrical stimulation in the lesion site could have an effect on the predominant HC rhythms in anesthetized rats. Voltage-controlled stimulation (pulse width 1 ms) in the MS site was performed in the range of 5 to 10 V at a 10 Hz frequency. Electrolytic microlesions were made by passing 200 μA DC current for 15 s. In post-lesion stimulation the same protocol was followed. We could elicit a high amplitude HC rhythm, phase-locked to the stimulation artifact and demonstrated it was not a part of this artifact. In the constructed multitaper spectra, we noticed a combined response of 10 and 20 Hz components. Based on this finding, we proposed an objective threshold measure and a loop in which the simultaneously enhanced harmonic influences the 10 Hz-enriched baseline resulting from stimulation. The lesioned rats also presented with a strongly elevated low frequency (1-4.8 Hz) contribution in the baseline, which was smaller in the control group. During stimulation, the lesion group displayed a steady amplitude rise across the stimulation intensities, while the non-lesion group's amplitude peaked at 6 V and then decreased. The presented acute focal lesion model could be relevant as a model for lesion restoration.

Abbreviations

Abbreviation	Explanation
ACh	AcetylCholine
ANOVA	ANalysis Of VAriance
AUC	Area Under Curve
BBB	Blood-Brain Barrier
CA1 CA2 CA3	Cornu Ammonis 1, 2, 3
DBB	Diagonal Band of Broca
DC	Direct Current
EB	Evans Blue
EC	Entorhinal Cortex
EEG	Electro-Encephalogram
(E)EMD	(Ensemble) Empirical Mode Decomposition
FF	Fimbria/Fornix
GABA	Gamma-AminoButyric Acid
HC	Hippocampus
ICA	Independent Component Analysis
IMF	Intrinsic Mode Functions
KA	Kainic acid
LFP	Local Field Potential
LIA	Low Irregular Activity
LTP	Long Term Potentiation
MR	Median Raphe
MS	Medial Septum
MWU	Mann-Whitney U test
PCA	Principal Component Analysis
PCPA	*p*-ChloroPhenylAlanine
PH	Posterior Hypothalamic nucleus
PPT	PedunculoPontine Tegmentum
REM	Rapid Eye Movement
RPO	nucleus Reticularis Pontis Oralis
RSA	Rhythmic Slow Activity
SAP	IgG-Saporin
S-HC	Septo-Hippocampal
SOBI	Second Order Blind Identification
SuM	SupraMammillary nucleus
VDB	Ventral Diagonal Band of Broca

Index

1. Introduction

One of the most prominent Local Field Potential (LFP) patterns that can be recorded from the rat hippocampus (HC) is a 3 to 12 Hz rhythmic slow activity, traditionally called 'theta rhythm'. These sinusoidal-like oscillations with amplitudes as high as 2 mV accompany voluntary movements such as walking or jumping, Rapid Eye Movement (REM)-sleep ('type 1 theta' or 'atropine-resistant theta') and are present during urethane or ether anesthesia and some states of immobility ('type 2 theta' or 'atropine-sensitive theta') (3, 4). The theta rhythm is believed to originate from brainstem structures as non-rhythmical discharges. In ascending to the HC via the supramammillary (SuM) nucleus, the posterior hypothalamic nucleus (PH) and medial septum (MS) these signals gradually adopt the correct frequency and amplitude (3, 5, 6). The amplitude and phase of the recorded theta depends on the exact electrode position in the HC, with the highest peaks in the Stratum Moleculare and Stratum Oriens and a 180° phase difference between these foci (7-11).

From the earliest experiments in the fifties it was clear that the MS has a leading role in HC theta formation and maintenance (12-14). An electrolytic lesion located in the MS - but not in the lateral septal area, the diagonal band of Broca (DBB) or the medial region of the fimbria/fornix (FF) alone- is capable of reducing the amplitude or completely abolishing theta rhythm in the HC (6, 10, 14-25). A complete elimination requires extended damage of the MS (16, 20). The lesions that caused a disturbance in theta rhythm are smaller, but always included the MS and often extended more deeply to the DBB (16).
Furthermore, the tight connection between MS and HC is also apparent in the 'driving' phenomenon (12, 26-28). Low frequency electrical MS stimulation in the theta range can evoke theta rhythm in the HC, phase locked to the stimulation pulses. Besides phase-locking, driven theta is also characterized by an amplitude increase and the appearance as similar waves. Though high-frequency stimulation blocks theta rhythm, it can still cause driving when leaving gaps at theta-frequencies or integer multiples of those gaps (26, 29, 30). The resulting power spectrum typically presents with a peak at the stimulation frequency and the first harmonic (5, 29, 31-39). The driving intensities mentioned in previous studies range from 0,5 V to 10 V and from 1 to 900 μA and depend on the animal (22, 26-28, 39-42). Regarding stimulation frequency, each animal also displays its own threshold parameters, but traditionally 7,7 Hz is proposed (26). The occurrence of driving lasts up to approximately 30 Hz, though Wetzel (42) reported that stimulating at frequencies outside theta range results in theta frequencies.
The elicited theta is highly similar to the physiological theta, with regard to frequency, wave morphology, amplitude and phase depth profiles (22, 28, 41, 42). It also causes acetylcholine (ACh) release in the HC (43) and mimics the response to atropine and urethane in the same way as natural theta does, implying that type 1 and type 2 theta can also be distinguished in this way (28). However, in freely moving rats the elicited theta is dissociated from normal behavior correlates (41). It was therefore proposed that electrical stimulation of the MS can indeed activate the theta-generating circuitry, but in a non-physiological way. A considerable amount of research about this rhythm has been conducted in rats and rabbits, though animals like cats, guinea pigs or mice are also used (for a discussion, see (7, 44)). Probably, there are no major differences between the species, since they are all capable of producing both types of theta. With the exception of primates, the correlation with ongoing behavior is

also present in all examined animals, but each species seems to have its own theta-related set of behaviors (7, 44).

The MS has been the location for either lesioning *or* stimulating to test the effect on HC theta. To assess the post lesion results, authors usually turned to freely-moving (16) or urethane-anesthetized rats which display a spontaneous rhythm (10, 21, 45), stimulated in another theta-eliciting brain region such as the PH (46) or implemented a bypass circuit (47). Taking advantage of the facts that small MS lesions can diminish and MS stimulation can evoke HC theta rhythm, we investigated the effect of intralesional stimulation on the elicited HC rhythm and evaluate it as an adequate model for lesion restoration. The effect of lesioning was previously typically assessed in terms of amplitude or spectral power. In cases when no complete abolishment of theta was obtained, a decreased amplitude (e.g. (14, 19, 45) or a reduction in spectral power in the theta range (e.g. (47)) were reported. For that reason, these measures were also included in the present work in order to examine if intralesional stimulation can alleviate potential amplitude reduction.

2. Literature Study

2.1. The septo-hippocampal system

2.1.1. The hippocampus

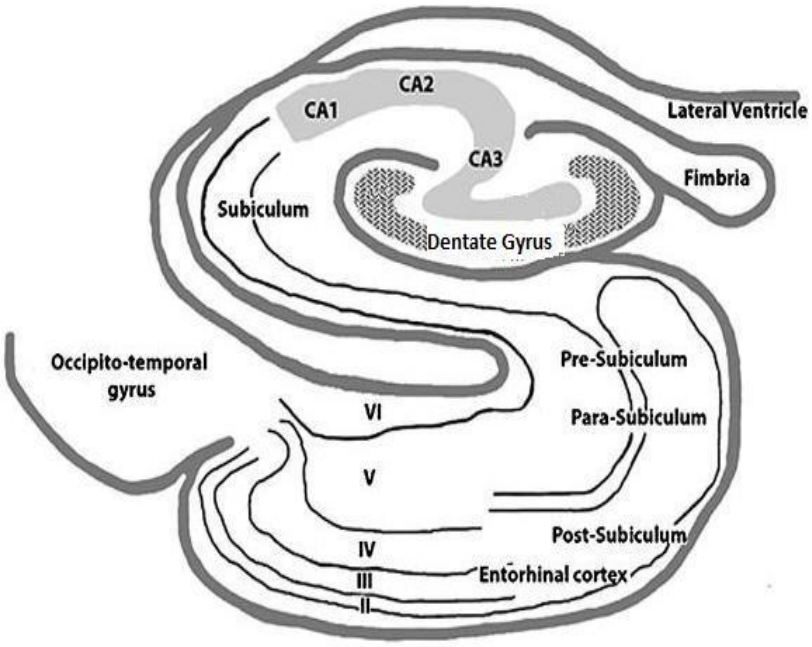

Figure 1. HC anatomy.
The HC comprises three regions: the dentate gyrus, the HC proper which is subdivided in CA1, CA2 and CA3, and the subiculum. Some authors also include the EC in the HC formation. Figure adapted from (2)

The HC comprises three cytoarchitectonically distinct regions: the dentate gyrus, the HC proper which is subdivided in CA1, CA2 and CA3, and the subiculum. It can be argued to include the entorhinal cortex (EC) in the HC formation (Fig 1). This structure also receives input from the MS, which causes it to produce theta activity (29, 48). The HC formation is organized in unipolarly connected zones, which not only include projection cells (pyramidal and granular), but also interneurons (for example basketcells). The latter can provide recurrent and feed forward inhibition: two processes important for production of rhythmical activity in the HC and EC (29).

Cell populations in structures, such as HC, the MS/DBB, EC and the median raphe (MR), exhibit discharge properties closely related to HC theta activity. These theta-related cells can be classified as 'theta-ON' and 'theta-OFF' cells. The first represent cells that increase their discharge rate during theta activity, while the latter display a co-occurring decrease in discharge rate. Both cells can have phasic or tonic subtypes, the difference being a consistent or non-consistent phase relation to theta field activity respectively (3).

2.1.2. The medial septal region

The medial septal region, located in the basal forebrain, has the shape of an inverted Y and includes a part on the midline (the MS) and an intermediate (vertical limb of the Diagonal Band of Broca (VDB)) and ventral part (horizontal limb of DBB) (Fig 2). Hence, it is frequently referred to as MS/DBB-complex (49). The integrity of this region is crucial for the generation of theta rhythm, as lesion studies show (cfr. infra).

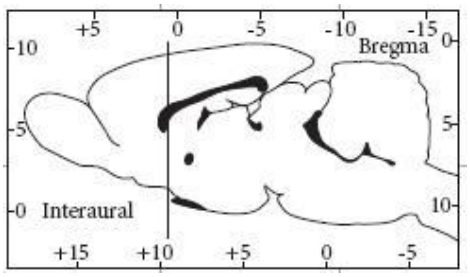

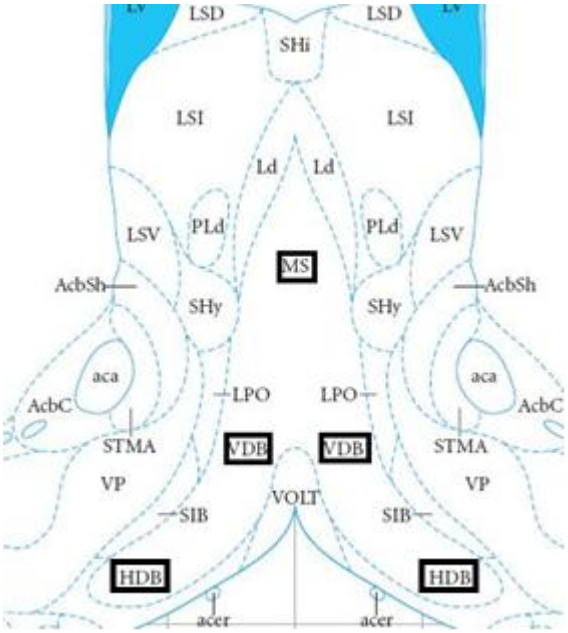

Figure 2. MS location.
The MS comprises three parts: medial septum (MS), vertical limb of the Diagonal Band of Broca (VDB) and horizontal limb of DBB (HDB). It is located in the basal forebrain. Figure adapted from (1).

The septum comprises at least three neuronal populations. Neurons using gamma-aminobutyric acid (GABA) and ACh as neurotransmitter have been described before (24, 48, 50-53), recently a third group of glutamatergic neurons has been identified (54, 55). The majority of projections from MS/DBB to HC are cholinergic (40-78%) and GABAergic (30-50%), versus approximately 20% glutamatergic (55, 56)). A significant portion of these septo-hippocampal (S-HC) neurons displays a rhythmical bursting activity, necessary for the generation of HC theta (13, 56, 57). The population of rhythmical bursting neurons, however, is heterogeneous. Selective cholinergic lesions considerably reduce, but not abolish their activity, suggesting that most of them are cholinergic (57). The other ones are proposed to be GABAergic (56). The fact that selective destruction of either GABAergic or cholinergic neurons significantly reduces theta rhythm indicates that both populations are important for its generation (45, 56, 58).
The function of the glutamatergic neurons requires still more research. Blockade of glutamate receptors on GABAergic and cholinergic MS/DBB neurons leads to a decreased firing, but did not affect their rhythmicity or HC theta. The results indicate that these neurons receive a strong glutamatergic input and can possibly be excited by glutamate receptors, even though these receptors are not crucial for production of rhythmic bursts in the septum (13, 59). When this activation of GABA and cholinergic neurons reaches a certain level, it may contribute to rhythm generation (59).

2.2. The hippocampal theta rhythm

2.2.1. **"Theta" as we know it**

Since Jung and Körnmuller (60) in 1938 first described this slow almost sinusoidal rhythm in the EEG of a rabbit and Green and Arduini (12) in 1953 first attempted to analyze it, the HC theta rhythm has been the source for many debates, resulting in a vast body of literature. Even the name 'theta rhythm' was a potential cause of confusion. In the earliest experiments, the frequency of the observed rhythm was in the range of the human EEG theta band (4-7 Hz). However, it is now clear that frequencies can vary between 4 and 12 Hz, depending on behavioral conditions and species. Therefore, theta rhythm is often referred

to as RSA or Rhythmic Slow Activity (29). Because this thesis involves rats, the described findings are focused on these animals.
Theta waves in the HC and other structures are recorded as an extracellular field potential with an amplitude up to 2 mV (3). The highest amplitudes are reached at the level of Stratum Oriens of the CA1 pyramidal region and Stratum Moleculare of the dentate gyrus, while a null zone is reported at the level of Stratum Radiatum. Below the null zone, the phase profile rapidly reverses causing the two foci of theta activity to be approximately 180° out of phase (7, 8, 18, 41, 61). Dentate theta has a slightly higher amplitude and remains in conditions where CA1 activity is absent (18, 61).
Frequently a point of discussion in theta terminology is the distinction between 'type 1' and 'type 2' theta, based on behavioral and pharmacological differences. Historically, the first is associated with voluntary behavior ('type 1 behavior') and is resistant to anticholinergic agents such as atropine sulfate, while the latter occurs during alert immobility and is abolished by equal doses of atropine or muscarine. The atropine-sensitive theta also occurs during urethane or ether anesthesia (9-11, 62). Kramis, Vanderwolf and Bland (4) originally defined movement-related theta as typically between 7 and 12 Hz and immobility-related theta between 4 and 7 Hz, though Gray and McNaughton (29) stipulate they cannot be distinguished by their frequency.
The distinction between the two types, however, is not as clear-cut as presented here. Movement and immobility related theta are not mutually incompatible (29). In the sensorimotor integration model Bland (3, 6) proposes type 2 theta always accompanies type 1 during voluntary movement, since he believes type 2 to be the electrical sign of processing the sensory stimuli relevant to the initiation and maintenance of voluntary behavior. Furthermore, both types of theta seem to have atropine-sensitive and resistant components (63) and type 1 and type 2 theta are not eliminated by selective lesions of cholinergic S-HC neurons (64, 65). Based on these and other discrepancies, Apartis et al. (57) plead for a reassessment of 'type 1' and 'type 2' theta, while Gray and McNaughton (29) suggest to abandon the idea of 'two types' and instead use the notion of '(at least) two gates' which may be separately or simultaneously open. Apparently, a serotonergic gate is open only during 'type 1' movement, while a cholinergic gate is open during both 'type 1' movement and theta-related immobility.

2.2.2. **On the origins of theta**

2.2.2.1. **The ascending pathway**

When the theta rhythm arises from the brainstem, it is still a collection of non-rhythmic neuronal impulses. In their ascension to the HC and neocortical regions, these signals then become rhythmic at the 3 to 12 Hz frequency (49, 56, 66-68). A multitude of structures display discharging neurons phase-locked to the HC theta waves. It is this series of 'oscillators' that contribute to the transformation of non-rhythmical inputs to a synchronized signal (49) (Fig 3). The origins of the ascending brainstem HC synchronizing pathways are believed to lie in the nucleus reticularis pontis oralis (RPO) (3, 56, 69). Bland et al. (66) showed that the administration of either electrical stimuli or the cholinergic agonist carbachol to this structure produced an intense activation of phasic and theta-ON cells in the MS and DDB. On the other hand, carbachol microinjections in the ACh-containing pedunculopontine tegmentum (PPT) are also capable of eliciting theta in the HC and at very short latencies in RPO. The authors concluded that this nucleus of the dorsolateral pons may

be a primary source of cholinergic input to RPO in the generation of theta (56, 70). To date, all studies demonstrated that discharges in the RPO and PPT nuclei are tonic, i.e. not rhythmically synchronous with theta (3).
The RPO sends fibers to MS, first passing through two structures in the caudal diencephalon: the SuM and the PH nucleus. Injections of carbachol or electrical stimulation in either of these regions drive theta-ON cells in both MS and HC and, additionally, increasing SuM/PH stimulation intensity linearly increases the discharge rate of septal and HC theta-ON cells (56, 66, 71-73). Electrical stimulation of the PH has been shown to activate the discharges of theta-ON cells and suppress those of theta-OFF cells, in both HC and MS/DBB (71). Kirk and McNaughton (74) found that procaine injections into the SuM decreased both frequency and amplitude, while MS injections only caused a reduction in the amplitude of RPO-elicited theta. They suggested that the *frequency* of theta rhythm is encoded in the SuM, rather than in the MS/DBB. The tonically firing PH cells and the SuM neurons, which discharge rhythmically phase-locked to theta, may act synergistically to relay RPO signals to the MS/DBB (56).
Next to these synchronizing pathways, there is also a desynchronizing pathway that functions as the theta off switch (Fig 3). The termination of theta rhythm is mediated by pathways originating in the serotonin-containing nucleus of the MR. Experiments in anesthetized rats showed that electrical stimulation of the MR caused desynchronization in HC field activity (3, 75), while lesions resulted in a constant release of theta (3, 76). Interestingly, in freely moving rabbits a similar electrical stimulation not only disrupted HC theta, but also the discharges from MS cells, while MR suppression resulted in an increased frequency and regularity of rhythmically discharging MS and HC neurons as well as a steady HC theta activity (77, 78). Given the MR stimulation effect on MS cell activity, a pathway for the modulation on HC activity going through the MS is suggestive (3, 79).

2.2.2.2. **The MS**

The MS acts as a switchboard for the incoming signals of the ascending pathways, distributing them to the posterior cingulate cortex, EC and HC (3). The HC and the septal region are tightly interconnected through the FF system. Theta in the dorsal HC depends on fibers travelling in the fornix superior, while the ventral HC depends on fibers travelling in the fimbria (17, 29). The S-HC projections should be regarded as a three-neurotransmitter pathway with cholinergic, GABAergic and glutamatergic components (49). Cholinergic S-HC neurons synapse with both HC principal cells and interneurons, contrary to GABAergic neurons which only synapse with interneurons (50). The target neurons of the glutamatergic pathway or its role in theta generation is still under debate.
The cholinergic projections are excitatory, however there is almost no evidence supporting a phasic excitation of principal cells as the theta inducing mechanism. The current hypotheses point to multiple coexisting influences from the septum as discussed by Stewart and Fox (11) and Gray and McNaughton (29). The proposed integrated model by Colom et al. (49) starts with afferents from SuM and PH that establish excitatory synapses with cholinergic and GABAergic septal neurons. The glutamatergic projection neurons are activated by and work together with the S-HC cholinergic neurons to initiate theta oscillations in HC networks. When this excitatory background reaches a critical level, the theta rhythm materializes in local septal, S-HC and intra-HC circuits.
In the septum the theta oscillations are facilitated by cholinergic and excitatory glutamatergic neurons that activate GABAergic interneurons and projection neurons. These

inhibitory neurons provide feedback for the excitatory neurons. It is this balance between the excitatory and inhibitory systems that determines whether theta or low irregular activity (LIA) occurs (6). At the level of the HC, principal neurons generate a depolarized state through the excitatory inputs from MS/DBB, which is carefully regulated by the HC inhibitory interneurons, the so-called 'theta-OFF' cells (31, 49, 66).

In literature, the MS is frequently referred to as 'the pacemaker' of the HC theta rhythm (for example, (23, 37, 80)), which implies in the strictest sense that rhythmic inputs from the MS generate the rhythmic activity in the HC. In favor of this view is the fact that many MS cells fire rhythmically and MS lesions abolish theta rhythm in HC (cfr. infra). However, this strict interpretation of the 'pacemaker' hypothesis is not tenable anymore. One piece of evidence is that the injection of the cholinergic agonist carbachol in isolated HC slices (81) or together with the GABA-antagonist bicuculline in a septally deafferented rat (82) can produce theta in the HC. If not a pacemaker, then what role does the MS play in theta production? According to the most recent findings, it is believed that the MS directly modulates the *amplitude* of theta and secondarily translates the ascending brainstem information into the correct theta frequency (3, 5, 6).

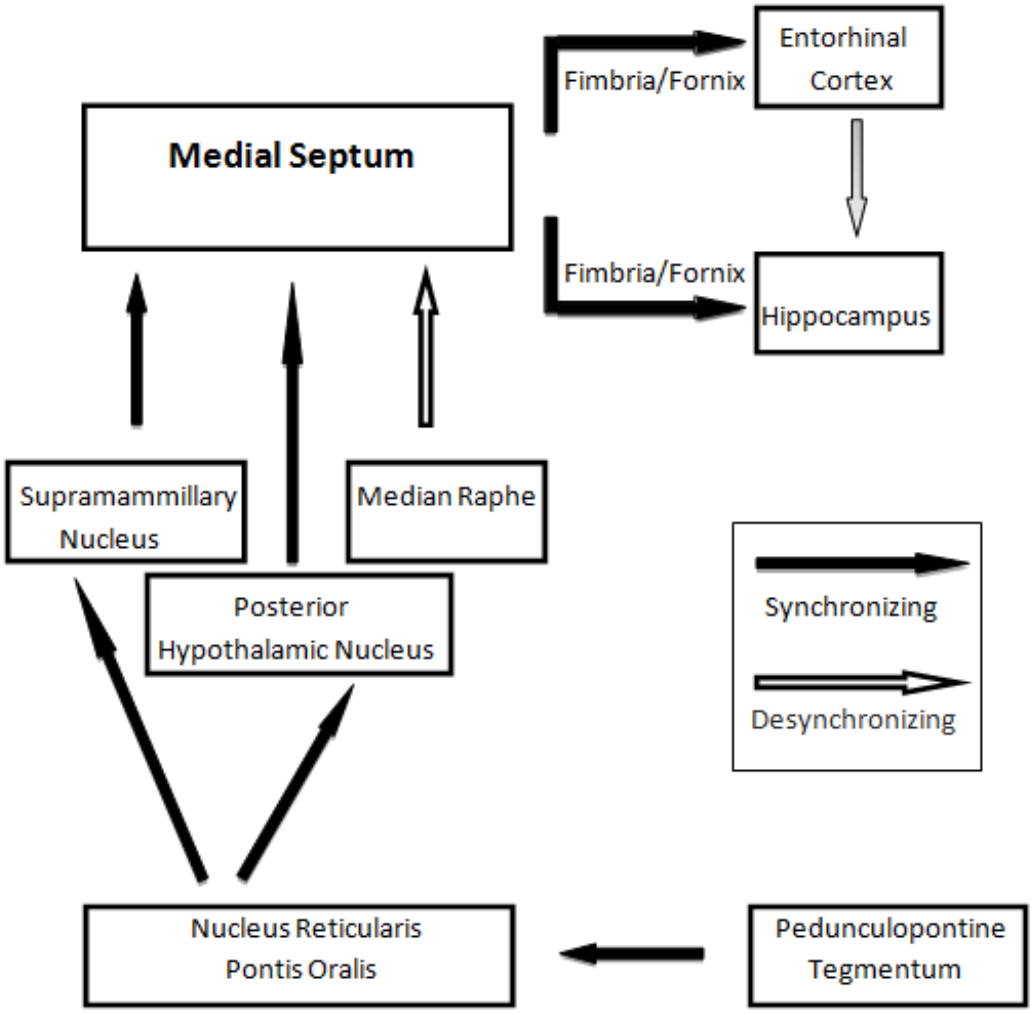

Figuur 3. The ascending pathway.
Theta originates from brainstem structures as non-rhythmic pulses. In ascending to the HC, it gradually adopts the correct frequency, i.e. synchronization. There is also a desynchronizing pathway mediated by the MR that terminates theta.

The MS/DBB complex also relays the information from the ascending synchronizing pathway to the EC. In this region, capable of independently generating theta (6, 66), the presence of theta-related cells have been documented by Dickson et al. (83). They could divide the EC cells related to HC theta field activity in theta-ON/OFF on the one hand and tonic/phasic on the other hand. MS lesions resulted in a loss or decrease of EC and HC theta rhythm, as well as a diminishment or depletion of acetylcholinesterase staining. Mitchell et al. (14) conclude that the MS probably also paces EC theta rhythm, presumably through cholinergic projections.

2.2.3. **Pharmacology of septal driving of theta rhythm**

The atropine-resistant form of theta (type 1) is unaffected by any cholinergic manipulation and occurs during type 1 movements. It is, however, sensitive to ether, urethane, chlorpromazine, reserpine, phenyclidine and entorhinal lesions (84). The non-cholinergic theta is presumably serotonergic in nature as is demonstrated by Vanderwolf and Baker (85). They reported that *p*-chlorophenylalanine (PCPA), a tryptophan hydroxylase inhibitor, preventing the synthesis of serotonin, in combination with atropine could attenuate or eliminate theta. The fact that increases in serotonin through MAO inhibitors, or by stimulating the MR, one of the main sources of serotonergic fibers, concomitantly increases in type I behavior and atropine-resistant theta supports this theory (86). Lesion experiments suggest that the atropine-resistant theta is mediated by a diffuse pathway, which traverses the hypothalamus, cingulate and neocortex before reaching the HC via the EC (87).
The atropine-sensitive or type 2 theta can be enhanced or made to occur during type 2 behavioral immobility by the systemic application of cholinergic agonists such as eserine (84, 88). Conversely, systemically given antimuscarinic drugs such as atropine, scopolamine or quinuclidinyl benzilate, destroy all theta in anesthetized rats. In waking animals, any theta that is elicitable during type 2 behavior, with or without eserine-treatment, can similarly be abolished by antimuscarinic drugs (84). This cholinergic theta is presumably mediated through the MS/DBB inputs to the HC, although some evidence suggests a minor cholinergic pathway, originating in the magnocellular pre-optic area, enters the HC through the EC (84, 89).
A substantial part of research on theta rhythm has been performed in animals anesthetized with urethane. If the level of anesthesia is carefully controlled, this drug evokes a theta rhythm in HC. Lighter doses typically produce an alternation between theta and low irregular amplitude (LIA) (41). With higher doses, theta generation is still possible, but only after sensory stimulation (i.e. tailpinch) (5). Atropine completely abolished all theta activity, categorizing it as a type 2 rhythm (4). Consequently, urethane and atropine administered together should block both the cholinergic and serotonergic form of theta, attributing the remaining theta to a third neurotransmitter system. Smythe, Colom and Bland (90) identified a GABAergic participation in theta generation.
Smythe et al. (72) showed in urethane-anesthetized rats that a reversible blockage of the MS/DBB with the anesthetic procaine abolished both spontaneous and PH stimulation-induced theta in the HC. During the suppression phase the discharges from theta-ON cells were significantly reduced, while theta-OFF firing was unaffected. In parallel, the inhibition of theta-OFF cells that is normally produced by PH stimulation, was also abolished.

2.2.4. **Effect of lesions in the MS**

Lesioning is a frequently used tool in exploring the connections necessary for theta rhythm generation and the role it plays. Theta rhythm is dependent upon the integrity of the MS. Lesions in this region abolish or reduce the amplitude of theta field activity in the HC (6, 10, 14-24). The residual theta after a lesion also shows a reduction in the dominant frequency (16). While damage to HC afferents from the septum eliminates theta, damaging the feedback efferents does not. Rawlins et al. (17) demonstrated this by interrupting the feedback loop at the level of the fimbria or lateral septum.

A median lesion in this area eliminates theta in both hippocampi (88), while small lesions at the S-HC border, destroyed theta activity ipsilaterally. Andersen et al. (21) thus concluded that the fibers important for theta generation run through a bottleneck just behind the MS, emerging from the lateral part. A study mapping the critical region for rhythmic activity in HC theta cells using small electrolytic lesions, confirm this finding (25). It suggests that the MS/DBB complex is the single important area for survival of theta rhythm, since neither lesions in the lateral septal area, the DBB alone or the medial region of the FF have an effect. Furthermore, MS lesions also cause a reduction in the discharge rate of theta cells in type 1 behavior by 50%. Thus, the damage prevents HC theta cells from coding for movement or sensory processing, either by rhythmically firing or altering the discharge rate (25).

More recent studies investigated the contributions of specific neural populations on HC theta generation. Separate administration of kainic acid (KA), which preferentially destroys septal GABAergic neurons, and 192-IgG-Saporin (SAP), which selectively eliminates basal forebrain cholinergic neurons, under urethane anesthesia caused in both cases the disappearance of type 2 theta, whether it was induced by tail pinch, PH stimulation or systemic physostygmine. During movement, on the other hand, theta was only moderately reduced, suggesting that type 1 theta remained despite the loss of either MS populations. Nevertheless, the combination of intraseptal KA with intraseptal SAP lesions was still capable of eliminating movement-related theta (45). It should however be noted that KA lesions usually damage several neural populations (91). The exact contribution of septal GABAergic neurons (or the glutamatergic population) remains to be established although present studies suggest that both GABAergic and cholinergic septal neurons are necessary for theta under urethane anesthesia and contribute to movement-related theta (45, 49).

SAP lesions reduce the amplitude, but do not completely eliminate movement-related theta (65). Given both types of theta can occur during movement and the presence -though reduced- of theta activity after cholinergic lesions, GABAergic and cholinergic MS neurons may be responsible for distinct components of the movement-related HC activity (9, 45, 92). On the other hand, both populations could fulfill separate roles. GABAergic neurons may be primarily responsible for pacing the synchronization of HC theta while cholinergic neurons having the supporting role of amplifying the synchronization (11, 45, 65). In agreement with both ideas, lesions of both cell populations abolish theta during movement (93).

2.2.5. **Effect of electrical stimulation in the MS**

From the earliest experiments it was already clear that low frequency electrical stimulation with sufficient intensity in the MS can evoke theta rhythm in the HC (i.e. *driving*). Reported stimulation intensities range from 0,5 to 10 V and from 1 to 900 µA (22, 26-28, 39-42). High-frequency stimulation leaving gaps at theta-frequencies or integer multiples of those gaps -

which can produce theta frequencies as harmonics- have the same result (29). The use of continuous higher frequencies (75-200 Hz) blocks the effect (22, 42). The MS is thereby an exception, since most other brain areas require continuous high-frequency stimulation to evoke theta. In this case, theta frequency increases with higher stimulation intensities (37, 88). Brücke (22) shows the driving occurs because each subsequent stimulus progressively cuts down the elicited wave from the previous stimulus, causing the summation effect to occur at certain frequencies. The amplitude of the driven theta decreases, in general, with increasing stimulation frequency and is relatively constant. The lowest frequencies have the least constant amplitudes, because of the strong presence of slower background waves (22).
The study of the minimal stimulation intensity required to elicit theta for any frequency, typically produces a U-shaped curve in the freely moving male rat. The frequencies at the extremes (i.c. 10 Hz and 5,8 Hz) are the most difficult to drive, while intermediate frequencies are the easiest, with a threshold obtained at 7,7 Hz (26). The minimum in the curve can be shifted by application of different drugs (29). Several authors (22, 27) explored the frequency boundaries and found that a synchronous, phase-locked rhythm in the HC can be produced using frequencies starting from 4 Hz up to 30 Hz. Wetzel et al. (42), on the other hand, reported that 3-4 to 12-14 Hz stimulation frequencies are capable of driving, while a further rise in frequency (14-50 Hz) did not cause driving anymore, but produced HC theta frequencies in freely moving animals. The authors explained the reported high frequency stimulation up to 30 Hz to be the result of high stimulation intensities, combined with a short duration, and did not relate it to theta found in the naïve animal.
The elicited theta is highly similar to the physiological theta, with regard to frequency, wave morphology, amplitude and phase depth profiles (22, 28, 41, 42). Driving also causes ACh release in the HC (43). In addition, stimulation-induced theta mimics the response to atropine and urethane in the same way as natural theta does, implying that type 1 and type 2 theta can also be distinguished in this way. One type was abolished by atropine and occurred during spontaneous or urethane-induced immobility, like the atropine-sensitive theta. The other type was like the atropine-resistant theta unaffected by atropine administration and appeared after injection of this drug only when the animal was moving. Likewise, it disappeared with large doses of urethane (28).
There are, though, dissimilarities on a cellular level. The discharge properties of theta-related cells were different during MS stimulation-induced theta on the one hand and spontaneously occurring or PH stimulation-induced theta (41). These findings could be an explanation as to why in freely moving rats the elicited theta is dissociated from the normal behavior correlates (28, 39, 40) as opposed to the effects of PH stimulation (94, 95). Scarlett et al. (41) concluded that electrical stimulation of the MS indeed activates the circuitry involved in the generation of HC theta rhythm, but in a non-physiological way.

2.2.6. **Function and clinical relevance**

Theta was originally described as the HC arousal rhythm (12), but since then it has been implicated in a number of processes, including attention, general motivational changes, frustrative non-reward, information processing, learning and memory (7, 29, 96). A substantial part of the information about behavioral effects is gathered through lesion studies (for a discussion, see (29)). Winson (19) for example, abolished theta rhythm by an electrolytic lesion in the MS and found these rats were no longer able to perform a spatial

task. A deficit also seen in humans with HC lesions. Conversely, restoring theta-like rhythmicity can restore initial learning (47).
The functional importance of theta is also evident in long term potentiation (LTP). LTP appears to be highly sensitive to the phase of theta rhythm, with potentiation favored at the peak and depotentiation at the trough. This finding suggests a role for theta as windowing mechanism for synaptic plasticity (62, 97). In addition, theta seems involved in the neural coding of place information in the rat HC. As a rat traverses a place field, the HC place cells fire at a progressively earlier phase of the ongoing theta oscillation (62, 98).
There is evidence that S-HC oscillatory states, such as theta rhythm, play a role in the pathogenesis of epilepsy and can possibly have an antiepileptic action. The presence of theta seems to indicate a HC functional state in which production of seizures is inhibited. Seizures during theta-related conditions like wakefulness or REM-sleep or during spontaneous, tailpinch or chemically induced (carbachol) theta occur less frequently. In epileptic animals, the rhythmically bursting MS neurons display chronically increased firing rates, and decreased their firing rates immediately after HC epileptic discharges. It thus appears that inhibitory S-HC influences dominate during HC epileptic seizures. (99).
Theta rhythm can be recorded from the HC during type 2 or voluntary behavior (walking, running, jumping,…), but not during type 1 or automatic behavior (100). Moreover, theta seems to code for certain aspects of voluntary behavior. The frequency increases as the velocity of the movement increases (94) while the amplitude increases as the magnitude of the motor behavior increases (101). Oddie and Bland (69) provided more experimental data pointing to the theta involvement in the organization of motor behavior. An integrated sensorimotor model is proposed by Bland (3, 6). It illustrates how type 2 theta can occur in isolation, while there is always a co-activation of type 1 and type 2 inputs once voluntary (=type 1) movement is initiated.
Aside from the frequency, there do not appear to be major interspecies differences, except for primates. All of the animal species examined in (7) are capable of producing both atropine-sensitive as atropine-resistant forms of theta and display relations with ongoing behavior. Nevertheless, the neural systems underlying the production of theta are different. For example, some species (like rats) rarely show immobility-related theta, while others (like rabbits, cats, guinea pigs) do so often, especially in response to sensory stimuli, though all of them can produce it. Another nuance that has to be made is the fact that, even though in all species theta corresponds to behavior, there appears to be a distinct set of theta-correlated behaviors in each animal species (44). In the interpretation of the thesis results, we focused on rat data when available, and otherwise resorted to rabbit data, when they could be compared, with the knowledge of above mentioned small differences.
Finally, what about the ‘theta rhythm’ in humans? Implanted depth and surface electrodes have demonstrated a task-related high amplitude theta, which increases during verbal and spatial memory tasks (102). However, human theta cannot automatically be linked with ‘HC theta rhythm’ on the basis of frequency or its apparent relation to memory. First, investigation into the frequency and relations to behavior of human ‘HC theta’ must be conducted (29). In addition, human theta appears widespread over the neocortex instead of being restricted to the HC (102). Thus, more research in the occurrence of, for example, frontal pole theta and its relation to HC theta is required.

3. Experimental work

3.1. Materials and Methods

3.1.1. Animals

Experiments were conducted according to the applicable national and international regulations for treatments of experimental animals. The experiments were approved by the animal ethics committee of KU Leuven. 24 (Pilot N=10, Main N=14) adult male Wistar rats, weighing between 200 and 250 g at the time of delivery, were purchased from the animal facility of KU Leuven. Rats for the main experiment were in pairs randomly assigned to two groups: an experimental or 'lesion' group (N=7), undergoing the full protocol, and a sham-operated control or 'control' group (N=7), undergoing all steps of the protocol except for the induction of a lesion. For reasons of simplicity, the moment of lesioning in the experimental group and corresponding period in the control group will be referred to as 'lesion'. The same term without quotation marks points to the actual lesion in the experimental group.

3.1.2. Surgical procedures

The animals were anesthetized with chloral hydrate (0,5 g/kg). The body temperature was monitored with an anal probe feed-back controlled heating unit (WPI). Rats were fixed in a stereotactic frame (model 9000 Kopf Instruments) and the skin on the skull was incised. The bone surface of the skull was prepared and cleared. The wound was carefully rinsed with 0,9% saline solution. In the stereotactic frame bregma and lambda were leveled horizontally and a trephine opening was made in the medial part of the right parietal bone. Two Pt/Ir bipolar twisted wire electrodes (Plastics One, 250 µm internal diameter) were subsequently inserted through the exposed dura at following coordinates according to Paxinos' and Watson's stereotactic atlas (1): AP 0,5 mm, ML 1,2 mm, SD 6,2 mm for the stimulating/lesion electrode (MS site) and AP -3,3 mm, ML 2,2, SD 2,6 mm for the recording electrode (HC site).

3.1.3. Electrophysiological protocol

Brain activity was continuously monitored using a single channel head-stage amplifier (AM Systems, model 3000). LFP's were recorded from the HC site. The signal was filtered between 0,1 Hz - 3,0 kHz (band-stop 50 Hz), amplified 500 times and digitized with a mk1401 CED unit at 10 kHz. Signals were monitored, conditioned and stored using Spike2 software. Voltage-controlled electrical stimulation (pulse width 1,0 ms) was performed at the MS with intensities ranging between 5 and 10 V at a 10 Hz frequency. An electrolytic lesion was made at the same electrode by passing a 200 µA DC current for 15 s using a DS8000 pulse stimulator and iso-flex stimulus isolation unit (World Precision Instruments, USA). The optimal driving and lesion parameters were determined in a series of pilot experiments (N=10). When judging 'driving', three characteristics of the main response peak (i.e. the theta-peak) were evaluated: the phase- or time-locking to the stimulation artifact, the increase in amplitude and the similarity of the waveshape. In no case 4 V was enough to induce driving. The best stimulation frequency to elicit theta in the HC was shown to be 10 Hz, though the driving effect could be obtained in the range of 8 to 30 Hz. In order to avoid extensive destruction of the MS, those lesion parameters were chosen that had the lowest intensity (200 µA) and duration (15 s), but still displayed tissue damage.

3.1.4. **Experimental protocol**

After correct positioning of the electrodes, a stimulation test pulse of 1 V at 1 Hz was given and the occurrence of the artifact was verified on the screen. Next, a driving test pulse of 5 V at 10 Hz was applied and the elicitation of a response was visually confirmed. A pre-'lesion' recording of theta driving was then obtained in all rats. This consisted of a series of six stimulation sequences spaced by a 3 min stimulation-OFF period. Each run was characterized by a different stimulation intensity, randomly attributed from the values 5, 6, 7, 8, 9 and 10 V, with a fixed frequency of 10 Hz and duration of 6 s. Next, the experimental group received an electrolytic lesion in the MS with following parameters: 200 µA and 15 s. The sham-lesion group did not undergo any intervention during the same time-span. Afterwards, both groups were again subjected to their pre-'lesion' stimulation sequence. Finally, the position of the electrodes and extent of the lesion was histologically verified with Nissl (i.e. cresyl violet) staining, while the Evans Blue (EB) dye provided additional information on the damage to the BBB (Fig 4).

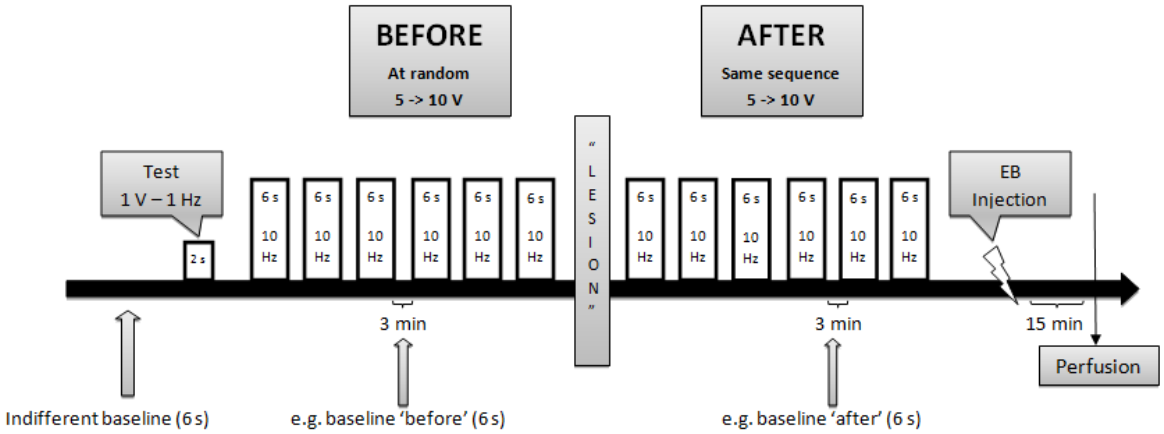

Figure 4. Experimental design.
After a test pulse, two series of stimulations were performed with random intensities in the range of 5 to 10 V. In between, the lesion group received an electrolytic lesion (200 µA, 15 s). After the experiment, EB was injected and the rats were euthanized and perfused. Indifferent baseline samples were taken before any stimulation; the other baseline samples were representative pieces, chosen in between stimulation sessions.

3.1.5. **Perfusion and histology**

After surgery 2% EB (0,2 ml)(Sigma-Aldrich, USA) was injected i.v. and allowed to circulate for ca. 20 min. This fluorescent dye is known to bind to serum albumin and is a marker for BBB permeability (103, 104). The animals were euthanized by CO_2 inhalation and perfused transcardially with a 10% sucrose followed by a 4% formaldehyde solution. The brains were removed and preserved in 4% formaldehyde until sectioning. Sagittal slices (50 µm) encompassing both electrode insertion sites were made using a vibratome (Leica, Germany). Three sections -each 600 µm apart- were mounted per slide. Next, adjacent slides were alternatingly stained with cresyl violet for anatomical visualization or cover-slipped for EB imaging. The location of extravasated EB on the sections was observed with a fluorescence microscope CellR (Olympus, Japan) at an excitation wavelength of 530-550 nm and an emission wavelength of >590 nm. Electrode and lesion positions were verified on the Nissl stained slides according to Paxinos and Watson's stereotactic atlas (1). For this, mounted

sections were first hydrated in distilled water, before transferring them to the cresyl violet solution (0,1%)(Sigma-Aldrich, USA) for a 4 min incubation. Afterwards, they were allowed to differentiate in acidified 70% ethanol and microscopically checked for optimal impregnation of the dye. The slices were then dehydrated by dipping in 90% and 100% and subsequently cleared in HistoChoice clearing medium (Sigma-Aldrich, USA) for 5 min. They were finally mounted using DPX Mountant (Sigma-Aldrich, USA) and coverslipped.

3.1.6. **Data analysis**

The LFPs were analyzed off-line with the Chronux package (105), a toolbox for signal processing of neural time-series data written in the Matlab scripting language (Mathworks, USA), and Ensemble Empirical Mode Decomposition/Independent Component Analysis (EEMD/ICA) (106). Response averaging, stationary and time-varying multitaper spectrograms were created with Chronux; signal deconstruction was performed with EEMD-ICA. The data encompassed all 6 s driving fragments, a representative 6 s part of the baseline before and after 'lesion' and a 6 s stretch of 'indifferent baseline', taken before the start of the 10 Hz stimulation series. Because we could not assume a normal distribution of the data, non-parametric statistics were used. For comparison of two independent samples, we applied Mann-Whitney U (MWU) tests. When comparing the groups to find differences in more variables, we resorted to multiple measures analysis of variance (ANOVA), lacking an adequate non-parametric alternative. Before applying ANOVA, however, we made sure the assumptions of homogeneity of variance (Levene's test) and normality (Shapiro-Wilk test) were fulfilled. For post-hoc analysis we used Tukey tests. All statistics were evaluated against a significance level α of 0,05.

3.2. Results

3.2.1. Histology

3.2.1.1. Nissl staining

Two rats had to be discarded from the dataset, because the stimulation artifact on the recording did not reach the expected height for the applied voltage and therefore the results were unreliable. Microscopic evaluation of the Nissl stained slices (Table 1 and Suppl. Fig 1) revealed that for all remaining rats (N=12) stimulation/lesion electrodes were positioned correctly in the MS. In approximately half of the cases the tip even extended into the VDB. The electrode track in the control group resembled a slim shaft (Fig 5 B,C,D), while the lesion group displayed a slightly larger damage at the end of the track (Fig 5 F,H). All but one of the recordings were obtained from the HC proper. In one rat the electrode was placed in the fimbria, the fibers connecting the HC and the MS. Most of the LFPs (N=8) were recorded from the Stratum Oriens layer in CA1 (e.g. Fig 5 A), two from CA2 (Stratum Lacunosum-Moleculare and Stratum Radiatum (e.g. Fig 5 G)) and one from the alveus (Fig 5 E) of the HC.

TABLE 1: Electrode location and polarity.

Animal	HC	MS
2112	Stratum Oriens	Top
0601	Stratum Oriens	Top
2701	Stratum Oriens	Deep to VDB
0102	Stratum Oriens touching Pyramidal layer	Top
0902	Stratum Oriens	Deep to VDB
1502	Fimbria	Deep to VDB
2212	Stratum Oriens	Deep to VDB
2601	Stratum Oriens	Top
0302	Stratum Oriens	Deep to VDB
0702	CA2/Stratum Lacunosum-Moleculare	Top
1002	CA2/Stratum Radiatum (close to Stratum Lacunosum-Moleculare)	Deep to VDB
1102	Corpus Callosum/alveus of the hippocampus	Deep to VDB

Grey boxes denote lesion group

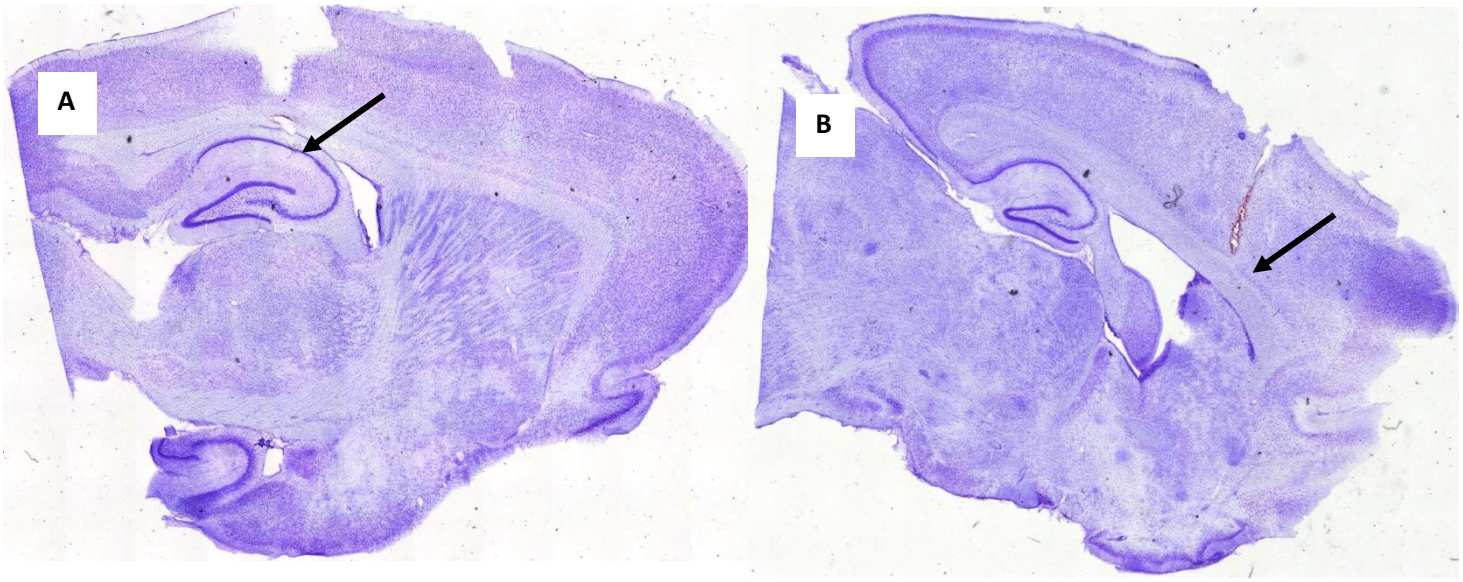


C

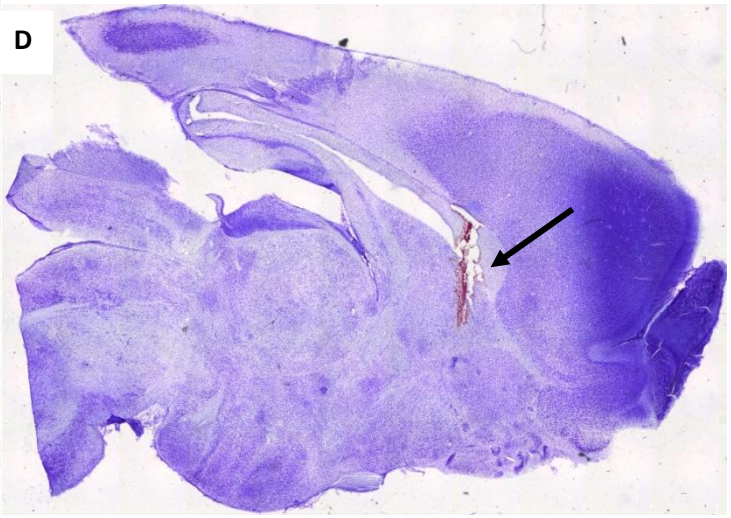
D

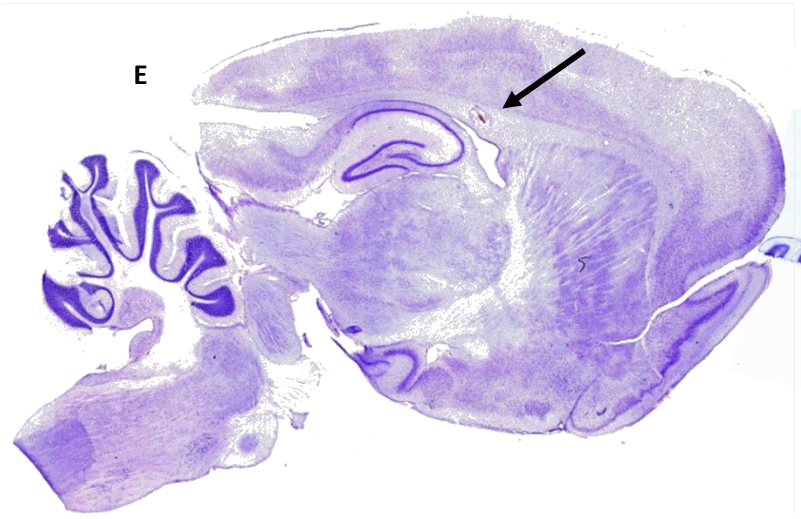
E

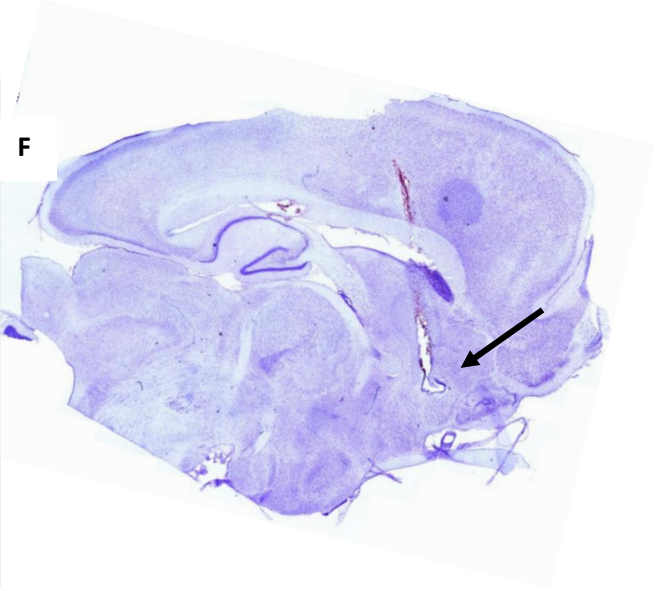
F

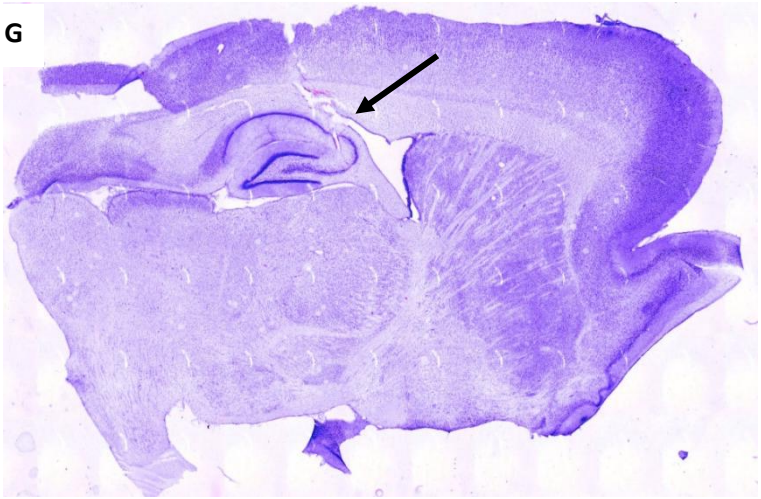
G

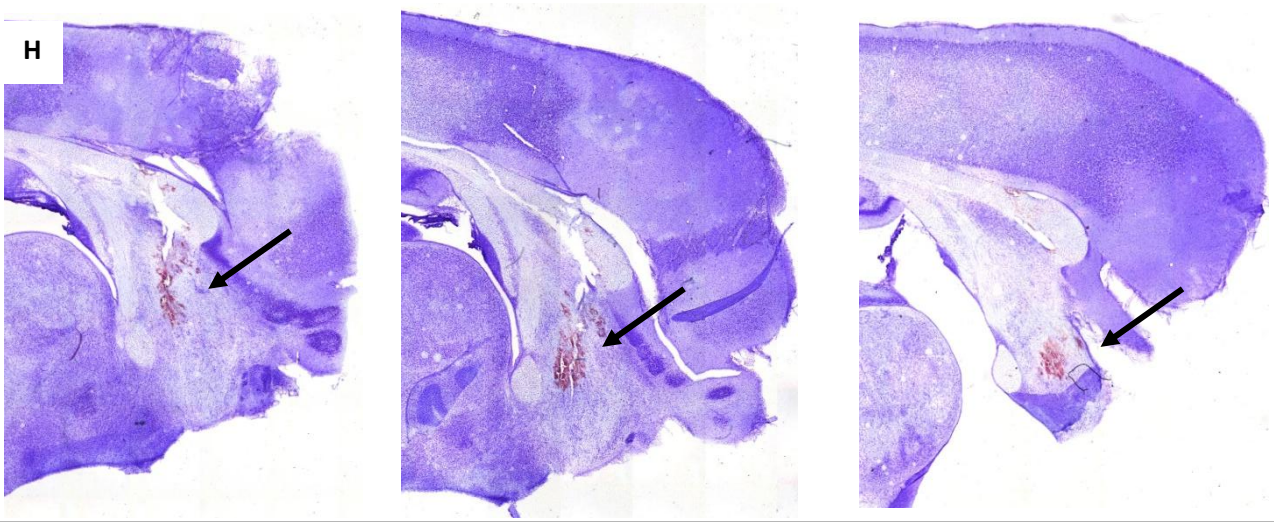

Figure 5. Nissl staining.
(A) Rat 0102 (control group). The recording electrode ended in the Stratum Oriens layer of the HC. (B-D) Rat 0102 (control group). The tract the electrode followed to the MS was clearly visible and resembled a slim shaft. (E) Rat 1102 (lesion group). The tip of the HC electrode remained in the alveus/corpus callosum. This particular slice also shows nicely the general anatomy. (F) Rat 1102 (lesion group). A rare example where HC and MS lesion are both visible n the same slice. At the end of the MS tract the damage is larger than in control rats. The same applies to the MS lesion (H) in rat 1002. (G) Rat 1002 (lesion group). The HC lesion in area CA2.

3.2.1.2. **Demonstration of damage to the blood-brain barrier (BBB)**

EB fluorescent microscopy provided us with additional information about the damage to the BBB and thus with a more extensive view on the total damage due to the intervention. The dye is taken up by endothelial cells, delineating the blood vessels, and by neurons in the neighborhood of the electrode tract (Fig 6 C). The EB signal expanded further than the actual tract and showed a certain directionality, extending the insertion trace (Fig 6 B,G). HC injuries typically had more clear-cut edges, while the ones in MS often had a 'fluffy' appearance in both groups (Fig 6 A,B,D,F,G). Based on the presentation of the MS damage alone, EB alone was not sufficient to distinguish between a lesion or control rat. Only a slight size difference could identify the microlesion. Lesion rats displayed marginally larger injuries than control animals. Another interesting fact we noticed in all imaged animals were EB positive granules in MS as well as HC sites (Fig 6 E,F). Furthermore, the closer to the electrode, the brighter the neurons lit up, suggesting the EB concentration gradient worked here longer than more distant. Comparing these findings to the ones from rat 1102 (Fig 6 G,H), which had an exceptionally short circulation time (approximately 2 min), could offer us some insight into the kinetics of EB. In this case the overall extent of the signal around the electrode tract was also more limited than in the other animals with intensities decreasing rapidly with distance from the electrode. Only few neurons were stained, indicating that it took more time for the dye to enter these cells. Conversely, the blood vessels were all clearly visible, suggesting that the dye was taken up by the endothelial cells almost instantaneously.

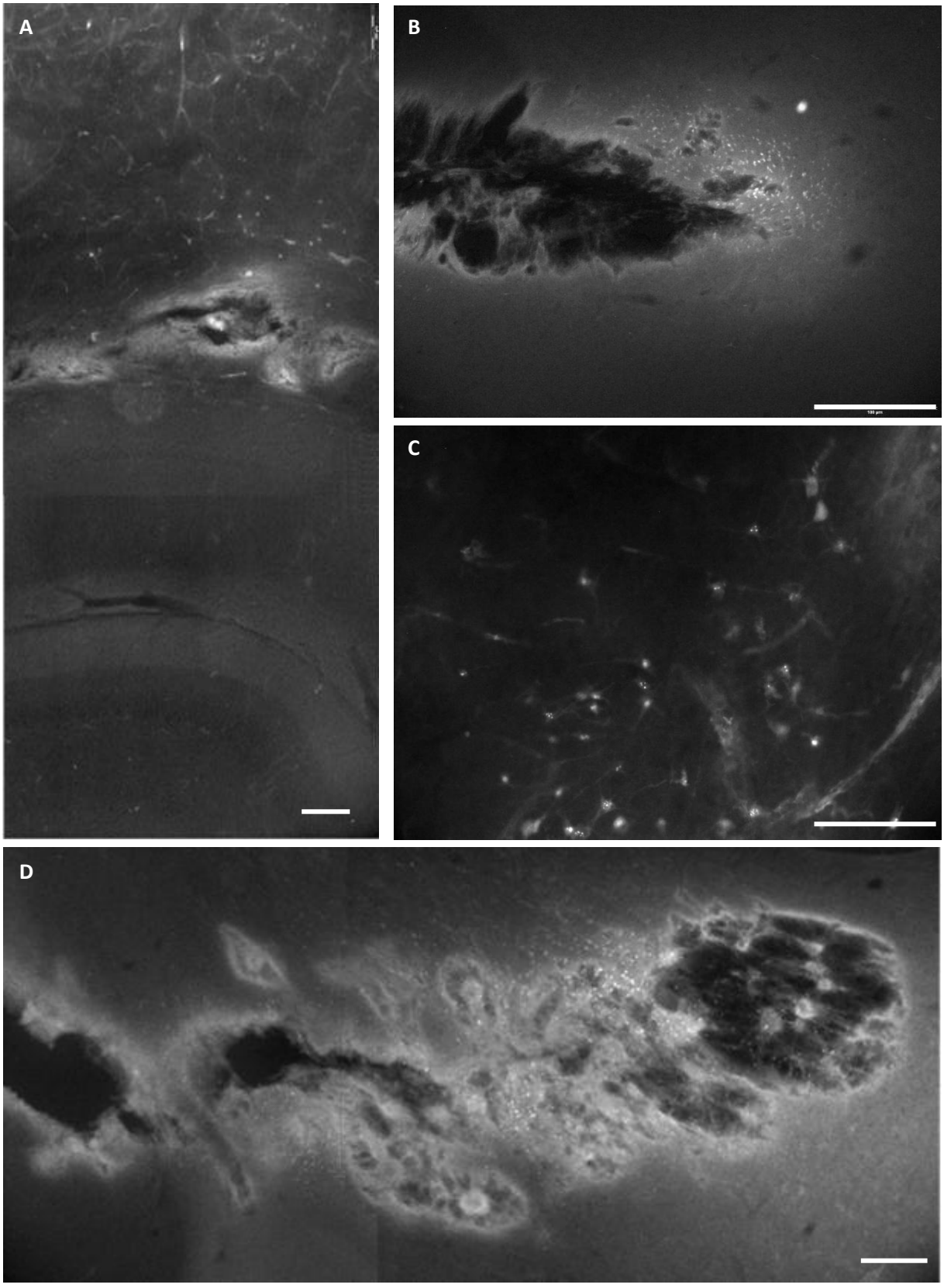
A
B
C
D

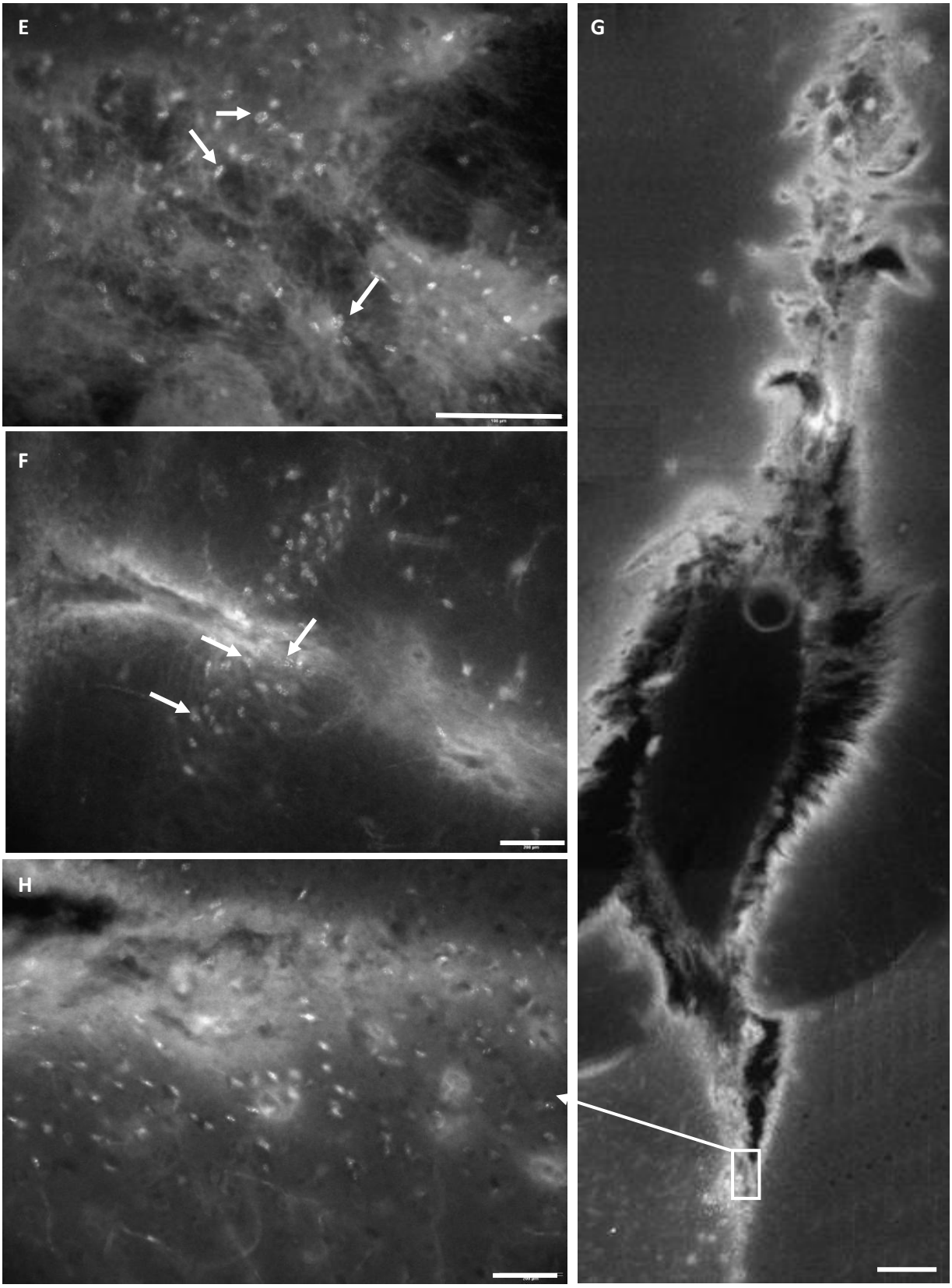

Figure 6. EB staining.
(A) HC and MS (B) electrode position in rat 0102 (control). The EB spread with a certain directionality, and entered neurons as well as endothelial cells (C). MS lesions in lesion group were slightly larger (e.g. rat 1002)(D). The presence of granules (arrows) were detected in MS (e.g. rat 0102)(E) and HC (e.g. rat 1002)(F) neurons. The EB signal in lesion rat 1102 (G and magnified in H) showed the intensity gradient with bright MS cells close to the tract and a weaker signal further away. White bars denote: 100 µm (C,F,G) or 200 µm (A,B,D,E,H)

3.2.2. **Observations from the recordings**

In all cases theta could be elicited before and after 'lesion'. The appearance of the evoked theta wave, though, was highly variable in different rats, especially in rats with suboptimal driving quality (cfr. infra). A large sharp peak either immediately followed the stimulation artifact or was first preceded by a small direct response (Fig 7 F). In some rats the main peak i.e. the largest deflection was negative (Fig 7 B), in others it was positive (Fig 7 A,F). Generally, this orientation did not alter in the same rat during the experiment. The peaks were usually biphasic or triphasic (Fig 7 C,D), but monophasic (Fig 7 B) forms sporadically occurred as well. Frequently, the waveform displayed serrations or small voltage changes within a single phase (Fig 7 A) and, occasionally, stretches of double peaks between two stimulation artifacts could be observed (Fig 7 E). All the described shapes could be found both before and after 'lesion', with no apparent difference between these two time periods or between control and lesion group.

During a single stimulation run, the high peaks were alternated by lower peaks. Though in general the average amplitude of the main peak either remained the same or started relatively high and decreased towards the end of the 6 s. For the greater part, amplitudes increased with higher voltages. However, each animal seemed to have its own optimal stimulation intensity which produced the largest effect and which appeared to be preserved after the lesion. When comparing 'after lesion' and 'before lesion'-periods, changes in amplitude were also observed regularly for equal voltages. Decreases and increases, however, were present in both control and lesion-group and in some rats the effect seemed mixed or no appreciable difference could be detected visually. Nevertheless, control rats usually displayed lower amplitudes over time, while the experimental group appeared to maintain the height of the main peak relatively well or even to increase it. Additionally, in nearly all cases a noticeable rise in background activity occurred in the 'after'-period. In time and thus with increasing stimulation sessions, the baseline became more 'irritated'. It displayed more and larger spontaneous peaks. These were observed independent from the direct 'theta-aftereffect', which was present for a few ms after the stimulation was terminated and usually when applying higher voltages.

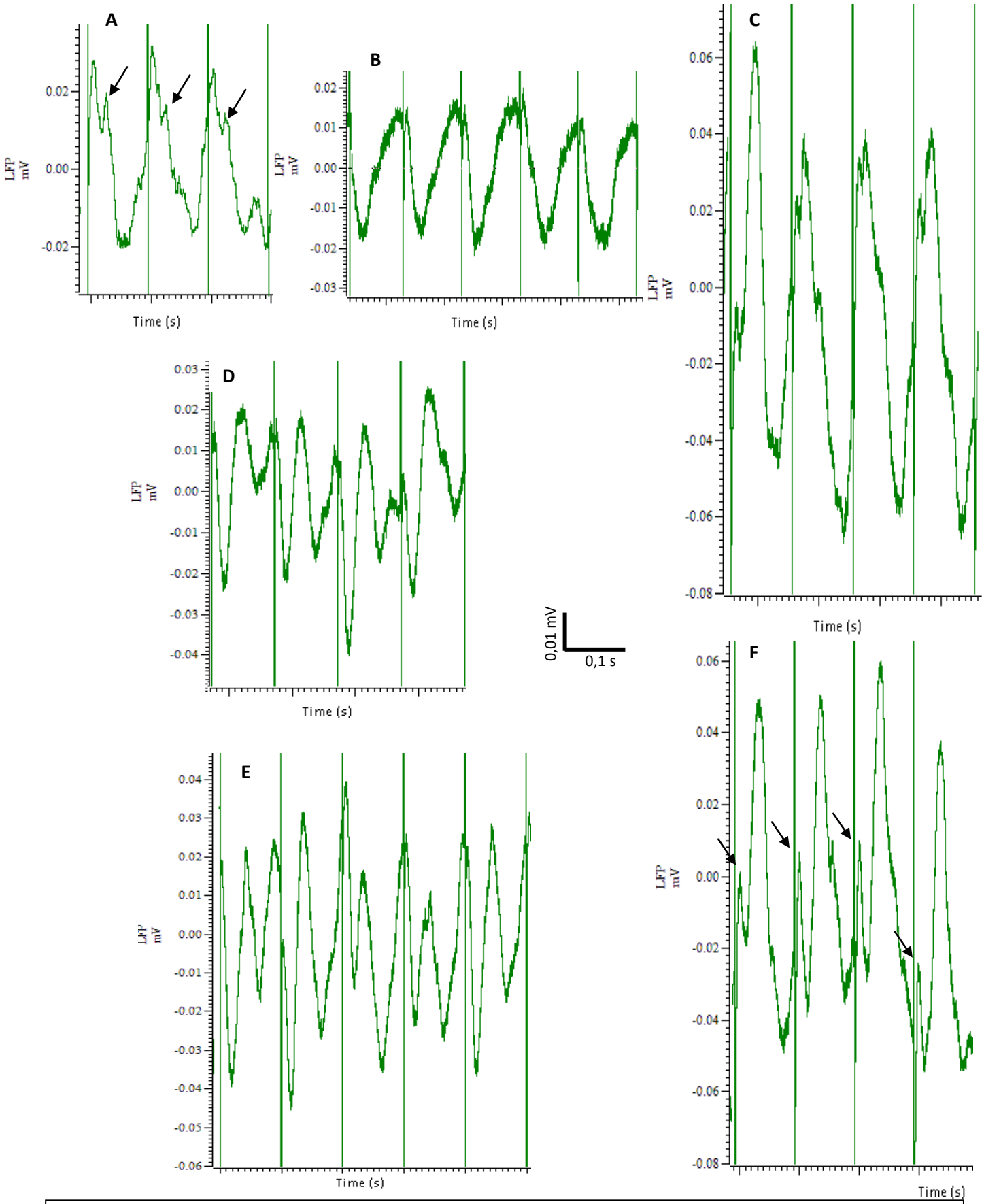

Figure 7. Theta wave presentations.
A grasp from the variety of manifestations of the evoked rhythm. (A) Rat 2212 (6 V, after lesion): serrations on the peaks (arrows). (B) Rat 0601 (9 V, after 'lesion'): negative, monophasic main peak. (C) Rat 2112 (6 V, after 'lesion'): biphasic peaks. (D) Rat 0102 (9 V, after 'lesion'): triphasic peaks. (E) Rat 0102 (9 V, before 'lesion'): double peaks. (F) Rat 2112 (8 V, before 'lesion'): the evoked potential peak (arrows) is clearly visible next to the main theta peak.

In a first exploratory approach, we evaluated the quality of the evoked theta driving by visually inspecting the recordings. First, for all rats a driving threshold was determined. This threshold was considered to be the lowest value at which phase-locking of a main peak and a minimal increase in amplitude, was clearly visible. In the majority of the cases, clear and sharp high amplitude peaks at equal distances from the stimulation artifact appeared already at 5V, but in four rats higher threshold voltages were determined (Table 3). After the 'lesion' moment, an identical average threshold was observed. The only difference being an elevation in one and a slight decrease in two cases.

TABLE 2: Quality of driving.

RAT	BEFORE	AFTER
2112	A+	A+
0601	A	A
2701	B	B+
0102	B	A
0902	D	D
1502	C	B
2212	A+	A
2601	B	C
0302	C-	C+
0702	B	A
1002	C	C
1102	B	B+

Grey boxes denote lesion group.
For definitions of A-D, see adjacent text.

Next, the animals were subdivided into four categories based on a subjective assessment of overall driving quality (Table 2). We took into account the three driving characteristics found in literature: high amplitude, phase-locking and similarity of the waves (3, 22, 26). Thereby is: (A) Clear and sharp single peaks with consistent phase-locking and high amplitudes throughout the voltage series (B) Mostly consistent phase-locking, mostly high amplitudes, appearance of double peaks and some irregular responses (C) The signal frequently escapes phase-locking, the response is frequently low in amplitude, peaks have a broad base and are frequently intermixed with irregular waveshapes (D) The signal remains small and irregular throughout the protocol. Even when a peak is observed, it has a broad base, low amplitude and frequently escapes the imposed 10 Hz of the stimulation. Because the variety in manifestations of the driving made it difficult to find a simple measure, we resorted to signal processing in order to obtain a more objective and quantitative criterion for driving quality and threshold.

3.2.3. **Non-stationary analysis and EEMD/ICA**

One piece of evidence that electrical stimulation resulted in a response in the theta range, is provided by the time-varying spectrograms. For these plots, a stretch of 50 s comprising one stimulation sequence was analyzed using the multitaper method in Chronux. The frequency limit was set to 50 Hz. The color-scale shows that during baseline recording low frequencies were most represented, especially <5 Hz (Fig 8). At a certain moment in time, the predominant frequency jumped to an averagely 10 Hz, with parallel a stronger signal in the 20 to 30 Hz band range as well. This 6 s stretch matched nicely with the moment of stimulation, while the high intensity at 10 Hz mirrored the stimulation frequency. What could also be ascertained from the non-stationary analysis, is the fact that in 'after' periods the theta frequency was more represented in the baseline than 'before'. This finding is consistent with the observation that the baseline became more 'irritated' in time.

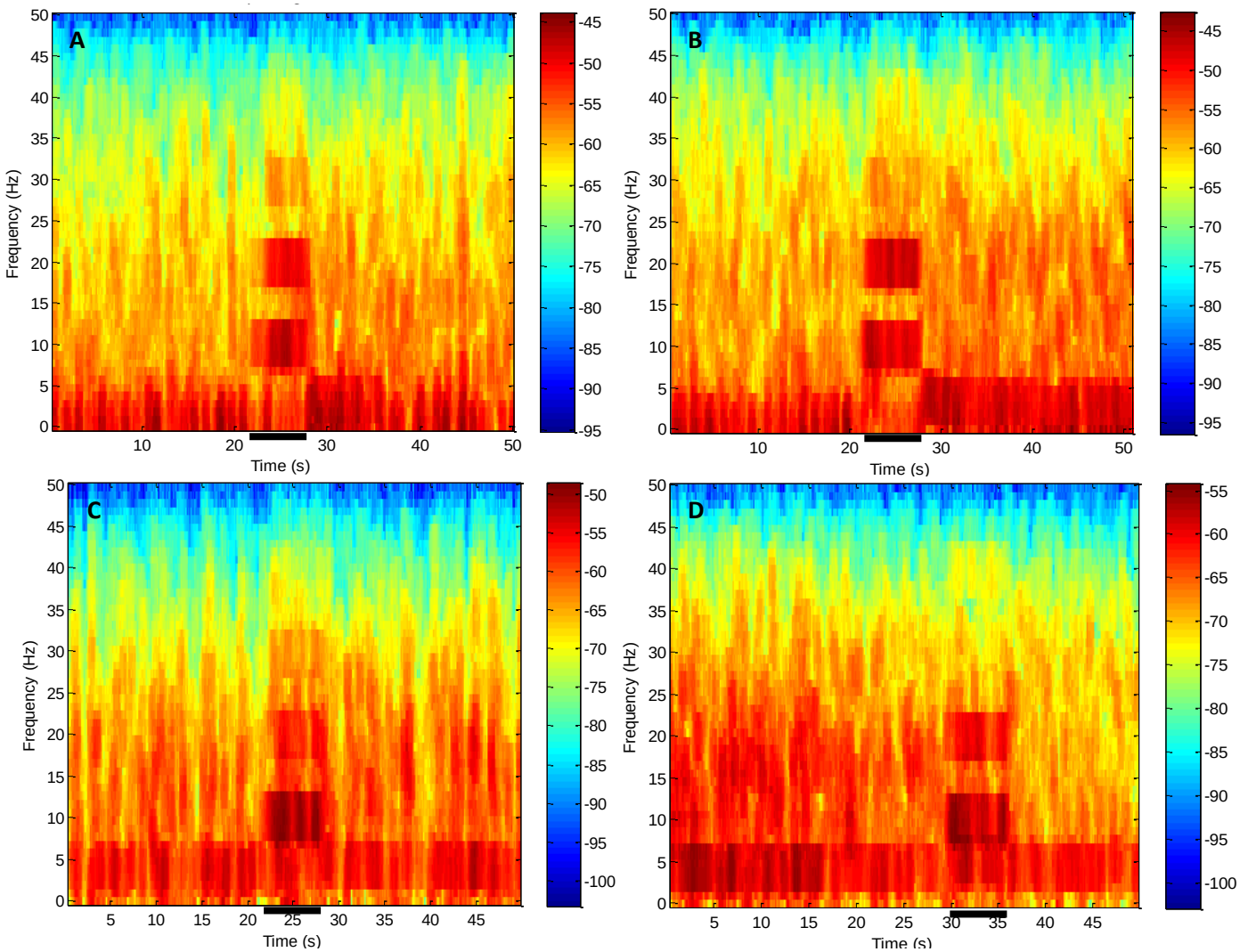

Figure 8. Time-varying spectrograms.
Rat 0702 (lesion group) before (A) and (B) after lesion. During the 6 s of stimulation, the 10, 20 and 30 Hz components are enhanced. Rat 2702 (control group) before (C) and after (D) 'lesion'. 10, 20 and 30 Hz components are enhanced, though the 30 Hz contribution disappeared in the 'after' situation. (Vertical bars denote stimulation period of 6 s. Color bar shows intensity of response)

We then applied EEMD/ICA (106) to determine if the observed response was an effect of the stimulation -and thus considered 'driving'- or rather part of the stimulation artifact. EMD is a technique that decomposes a time-varying signal into a finite set of oscillatory modes, the so-called intrinsic mode functions (IMFs). EEMD is a noise-assisted version of EMD and thus more robust. An extra denoising process was implemented by performing principal component analysis (PCA) on the IMFs prior to ICA. PCA reduces the most insignificant components of the data, retaining at least 95% of the original variance. ICA then extracts the statistically independent components ('sources') from a given signal. This approach makes it possible to reconstruct different spectrally overlapping processes that contribute to the overall observation.

Using Second Order Blind Identification (SOBI) (107) as a choice for ICA, and the PCA reduction of data to six components, we reconstructed the most important constituent (independent) sources of the signal. Among components, we searched for the one that had a peak and more than 20% of power located between 9 and 11 Hz. If this component also accounted for more than 25% of the overall signal power between 0,1 and 100 Hz, we

regarded it as the isolated rhythm of interest. In the case of stimulation, we detected a dominant rhythm of approximately 10 Hz in both lesion and control group, which was absent in the baseline fragments. According to this criterion, the isolated rhythm was always reconstructed successfully in the presence of stimulation, corresponding to the strong peak observed in signals' spectrum and visually matching the dominant oscillation in time domain (Fig 9 A,C,D). Peaks of this kind were observed only during stimulation and were not the part of the stimulation artifact, as was shown by a similar reconstruction (Fig 9 B). Since EEMD/ICA analysis demonstrated that the stimulation artifact only became influential at higher frequencies (Fig 9 B), the time-varying spectrograms (Fig 8) represent the induced signal alone with no contamination.

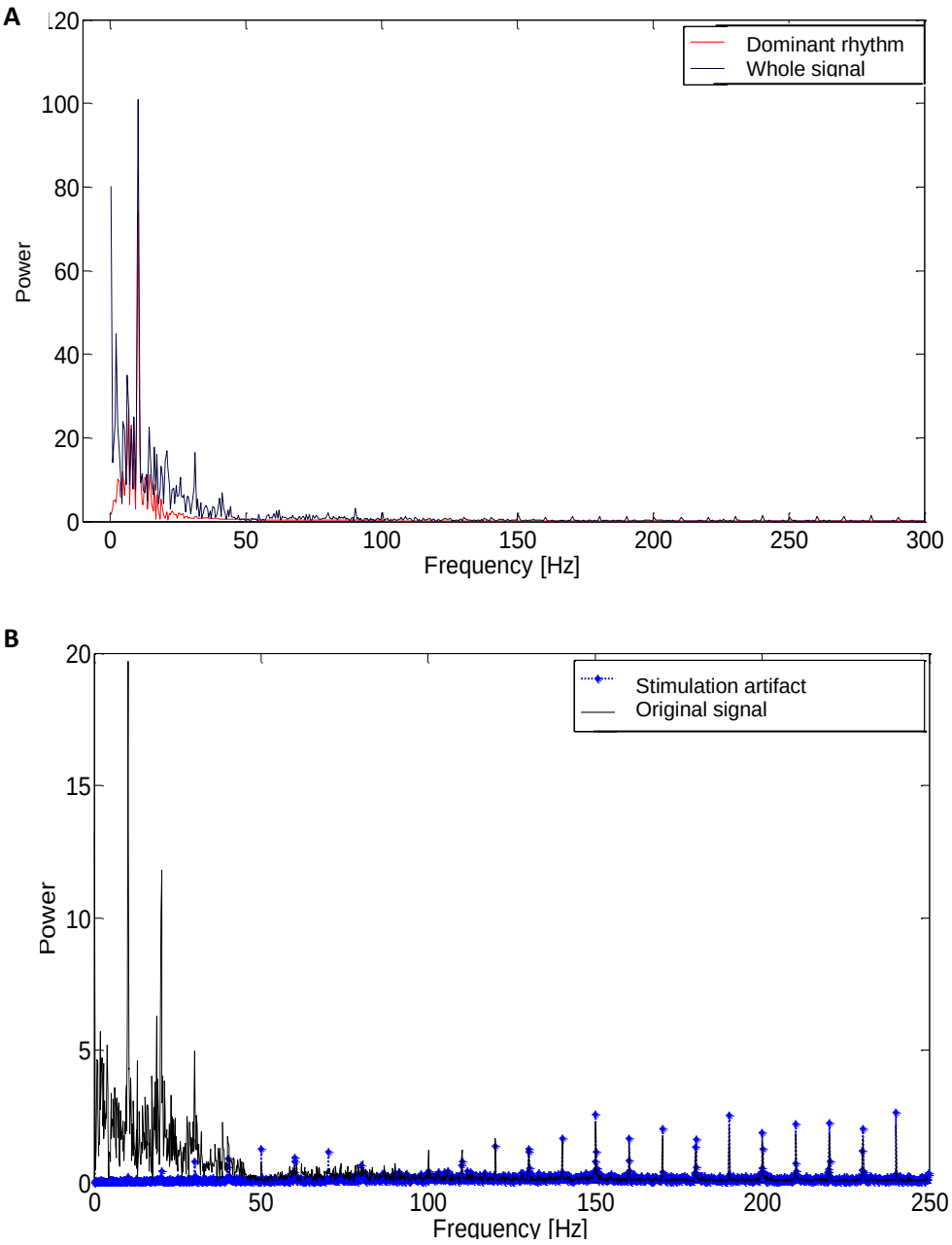

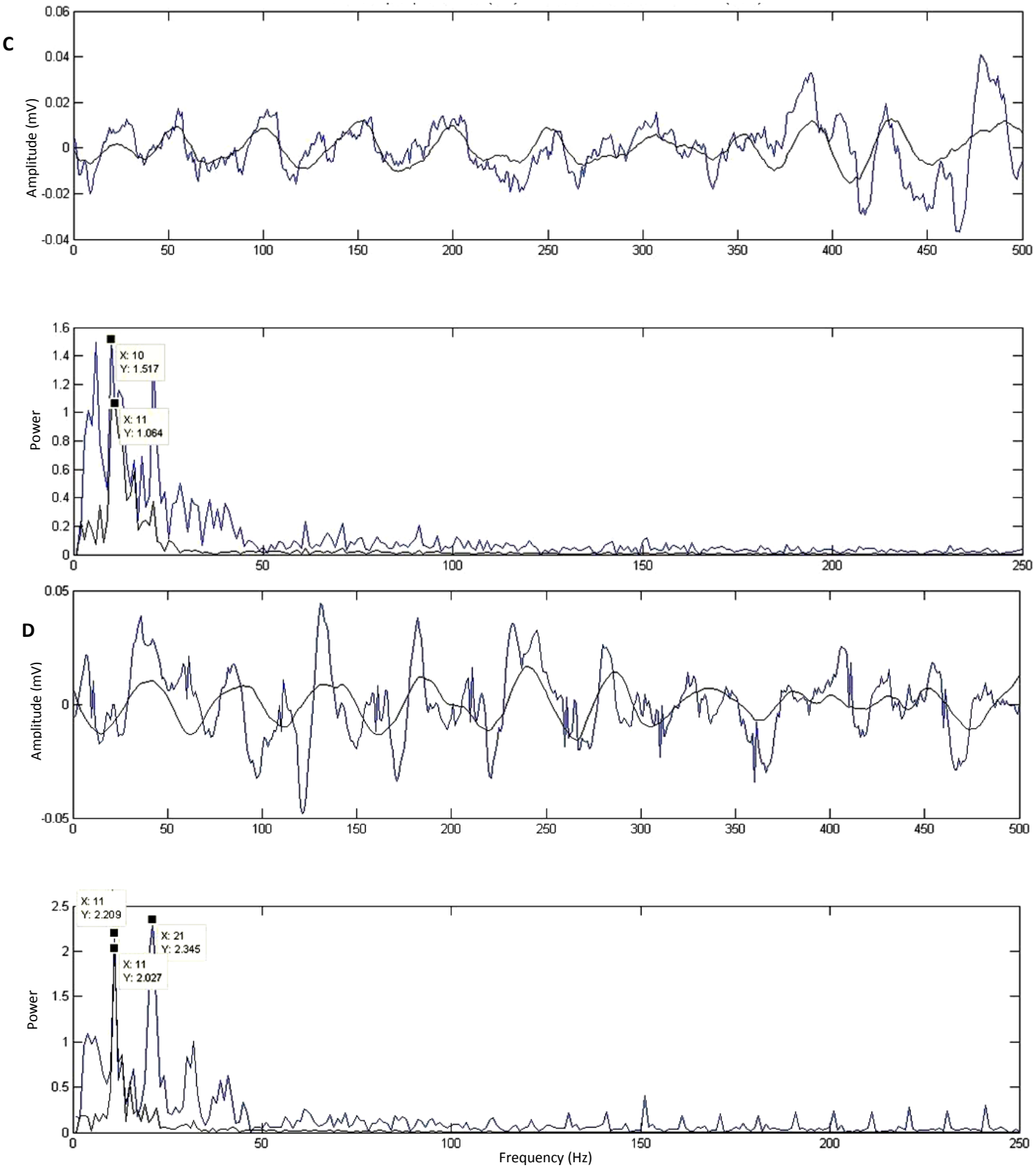

Figure 9. EEMD/ICA.
(A) Power spectrum showing overlap of the isolated dominant rhythm with the highest peak of the whole signal at approximately 10 Hz. (B) Power spectrum demonstrating that the signal of the stimulation artifact does not interfere with the signal of the evoked rhythm. Recording fragment (Top) and Fourier spectra (Bottom) during stimulation from rat 0702, 5 V, before (C) and (D) after lesion. In both spectra and recording fragments the reconstructed source (black) overlapped with the dominant component of the whole signal (blue) around 10 Hz.

3.2.4. **Spectral analysis**

3.2.4.1. **Description of multitaper spectrograms**

Next, we analyzed the data with Chronux software (105), which produced spectrograms based on the multitaper method. The majority of the power spectra derived from the driving fragments show clear, large and sharp peaks at 10 and 20 Hz (Fig 10 A-F) and sometimes a small peak at 30 Hz (Fig 10 E,F). In some rats these signals were either absent or too small to rise above the background activity (e.g. Fig 10 D), mainly at low voltages. Especially the occurrence of the first harmonic peak seemed relatively dependent on high stimulation intensities. Yet, it sometimes overpowered the theta response, like in rat 0102 (Fig 10 E,F), consistent with the observation of double peaks on the recording data in this animal (Fig 7 E). When comparing the before and after-'lesion' data, a change in the 10 and/or 20 Hz component was repeatedly observed. Although in both lesion and control group and at all intensities increases as well as decreases in the height of these peaks were present, the overall trend per rat was an increase. Only one rat (0902) displayed for theta and beta lower signals, three additional rats (0102, 2212, 2601) showed only lower beta peaks and two rats (1002, 2601) presented with a mixed result for theta, i.e. an increase for half of the voltages, a decrease for the other half. Subsequently, we ran the same script on all baseline data. None of the characteristic 10 and 20 Hz peaks observed in the driving fragments were present in these spectra. Furthermore, all spectrograms -driving as well as baseline- were marked by a prominent low frequency peak in the 1 to 4 Hz range.

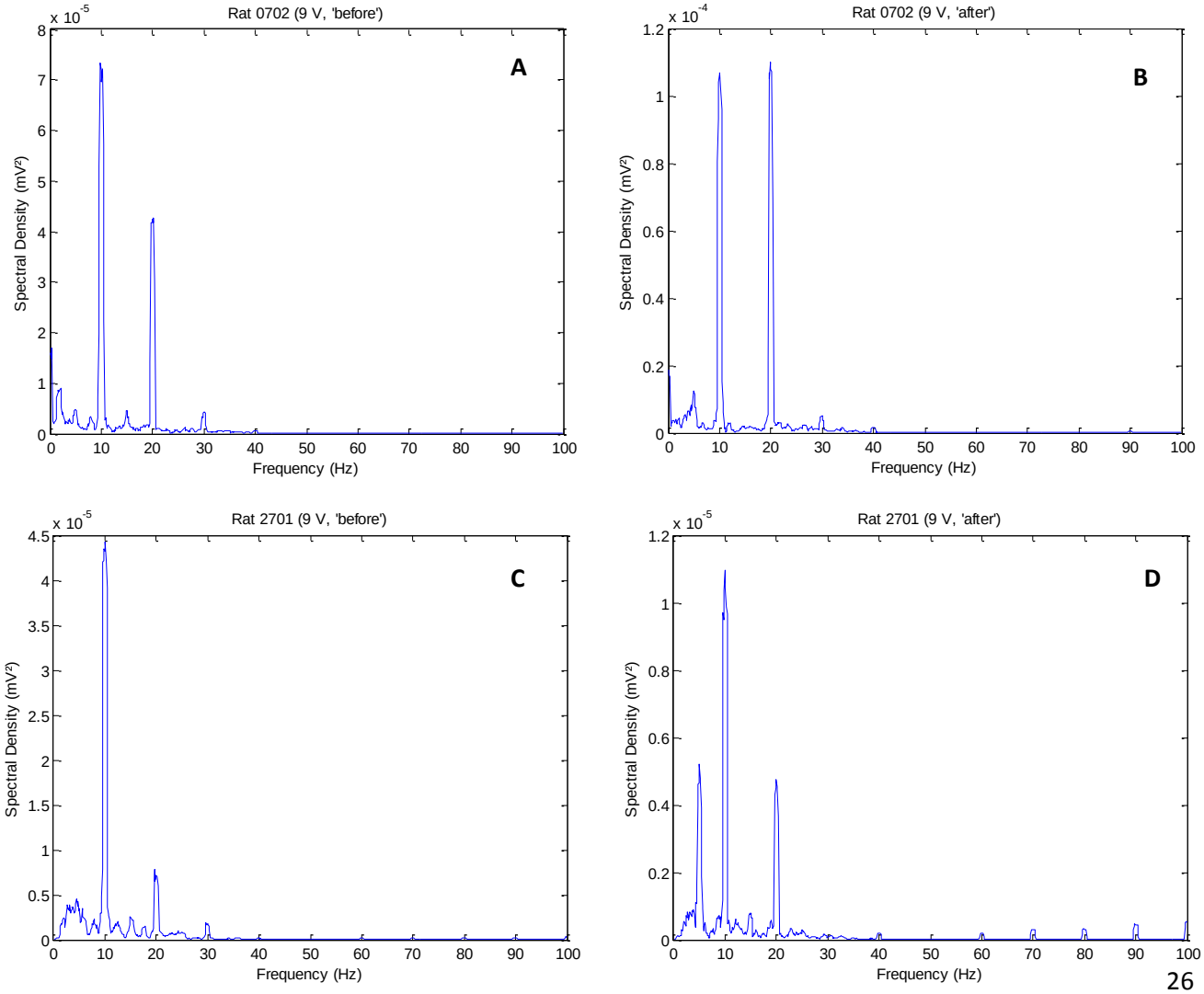

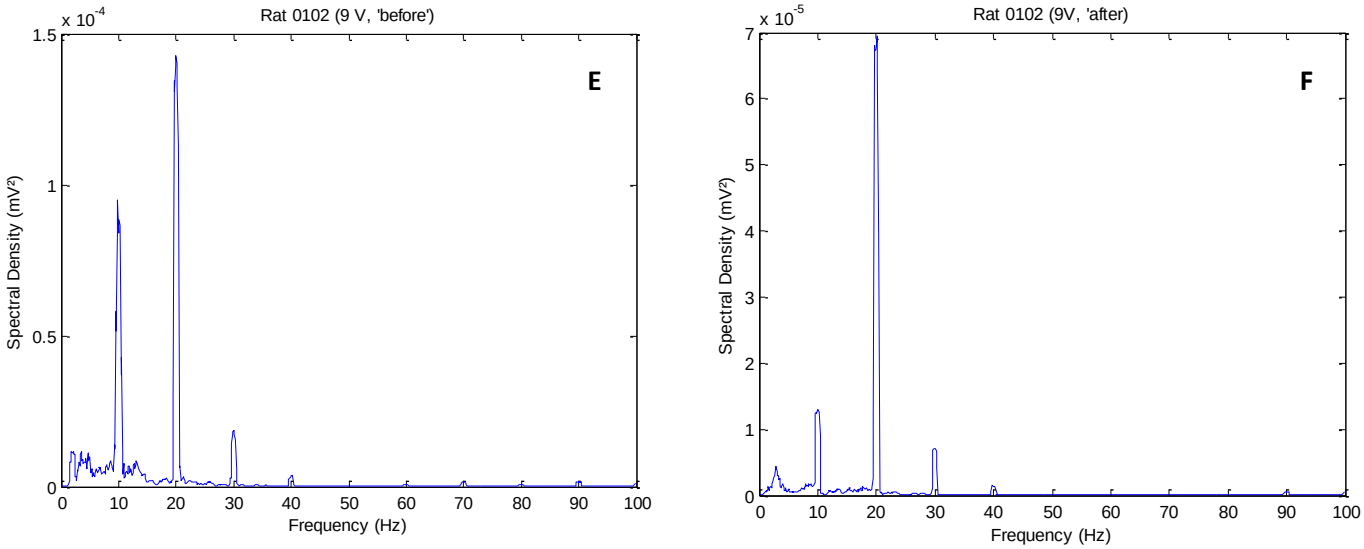

Figure 10. Multitaper spectrograms of driving fragments.
In both lesion (Rat 0702 (A) before and (B) after) and control (Rat 2701/Rat 0102 (C/E) before and (D/F) after) group, 10 and 20 Hz peaks are prominently present. Occasionally, a 30 Hz peak is also visible. In Rat 0102 the 20 Hz contribution even overpowers the theta 10 Hz, resulting in double peaks on the recordings. The low frequency peak in (D) illustrates the background enhancement after lesion (cfr.infra).

Next, we examined the contributions of the signal in five different frequency bands by calculating the corresponding area under curve (AUC). The following ranges were chosen to effectively isolate the described peaks in the spectra: “Low Frequency” (1,0-4,80 Hz), “Theta Low” (4,81-8,18 Hz), “Theta Driven” (8,19-11,82 Hz), “Beta Low” (11,83-17,99 Hz) and “Beta Driven” (18,0-22,0 Hz). The values 4,80 and 11,82 were obtained by averaging the lower and upper limits of theta rhythm respectively, as they are proposed for rats in different articles (Suppl. Table 4). Baseline fragments were simultaneously analyzed according to the same strategy. The resulting values appeared to be highly variable between animals, not only in magnitude, but also across stimulation intensities. The AUC maximum occurred at different voltages for different subjects, consistent with the before mentioned observation that the optimal driving intensity is individual.

3.2.4.2. **Determination of threshold and driving quality**

Based on the obtained dataset, we attempted to define an objective threshold for driving and find a measure for driving quality. Because the spectrograms indicated an important response in the 20 as well as in the 10 Hz component during stimulation, we utilized values from both frequency bands to factor in both contributions. We hypothesized that the higher the observed peaks rose above the background, the ‘better’ the driving was. Therefore, AUC’s of “Theta Driven” (θ(D)) and “Beta driven” (β(D)) in the situation before ‘lesion’ were summed and compared to the corresponding baseline value (Suppl. Table 1). If the summed result was 10% higher than the baseline, the signal was considered to be sufficiently separated from the baseline. Thereby also assuming that the larger this difference is, the better the driving quality. The lowest voltage at which the summed AUC value was above that mark was then considered to be the threshold. The 10% factor was arbitrarily chosen, though we believe it to be a reasonable measure for separating signal from background. Even though amplitude is an important aspect of driving, one must keep in mind that the subjective evaluation of threshold also takes into account other factors such as consistent phase-locking and waveshapes.

$$\sum \beta(D) + \theta(D) \geq 1.10 \sum baseline$$

Applying this formula, revealed a 5 V driving threshold for most of the rats, one at 7 V (0302) and in one rat (0902) the 10% level was not reached at any of the stimulation intensities (Table 3). We repeated the same procedure for after-'lesion' values and obtained a similar average threshold of 5,27 V compared to the 5,18 V from the pre-'lesion' period (MWU, 'before' vs 'after', p=0,47). Two animals needed a higher intensity of 6 V, rat 0302 on the other hand displayed a lower threshold of 6V and rat 0902 failed to attain the required 10% above baseline again. The remark has to be made that subject 1002 only passed the criterion at 5V, failing for higher intensities. This fact again corresponds well with the notion of an optimal driving intensity per rat. Finally, there appeared to be no difference between lesion or control group (MWU, 'Before' p=0,90, 'After' p=0,85).

Table 3: Threshold determination.

	Visual inspection			***Application of formula***	
RAT	**Before**	**After**	**RAT**	**Before**	**After**
2112	5	5	**2112**	5	5
0601	5	5	**0601**	5	5
2701	6	5	**2701**	5	5
0102	7	6	**0102**	5	6
0902	5	5	**0902**	>10	>10
1502	8	8	**1502**	5	5
2212	5	5	**2212**	5	5
2601	5	5	**2601**	5	6
0302	5	7	**0302**	7	6
0702	8	8	**0702**	5	5
1002	5	5	**1002**	5	5
1102	5	5	**1102**	5	5
Average	*5,75*	*5,75*	*Average*	*5,18*	*5,27*

Grey boxes denote lesion group

Overall, the subjective observations and the objective values (Table 3) obtained with the formula matched adequately. Threshold voltages from visual inspection were slightly higher for some animals than the ones based on AUC. In addition, the rats that previously were attributed with an A or B for driving quality generally also had the highest absolute AUC values. An exception was subject 1102 with relatively low values, although this was compensated for by the low baseline. On the other hand, subject 0102, an A rat, indeed had high AUC's, but an equally high baseline.

3.2.4.3. **Effect of 'lesion' on baseline**

Before looking into effects of 'lesioning' in the driving fragments, we examined potential changes in the baseline for all five frequency bands and compared both groups of rats. For most rats absolute baseline levels rose over time (Suppl. Table 2). Nevertheless, in none of the ranges, the AUC values displayed a significant difference between before and after

'lesion' moments. We then performed an ANOVA analysis on the ratio's of before and after values and compared them per group over all frequency ranges to examine whether the change in AUC between the two time points was significantly different in both groups. The results indicated that there was no difference between lesion and control group, but for the interaction of band range and group, the p-value was 0,001. Post-hoc analysis revealed that this significant value was situated in the lesion group, where the "Theta Driven" component in the baseline differed from the "Low Frequency" component (p=0,004). The same applied to the summed driven frequencies (p=0,04), which is probably due to the strong theta influence, since the 18 to 22 Hz frequency only showed a trend towards a discrepancy with the low frequency (p=0,053). A graphical representation (Fig 11) confirmed the sudden drop at the level of theta driven. Except for the stronger presence of the "Low Frequency" component in lesion rats, the graphs follow a similar path.

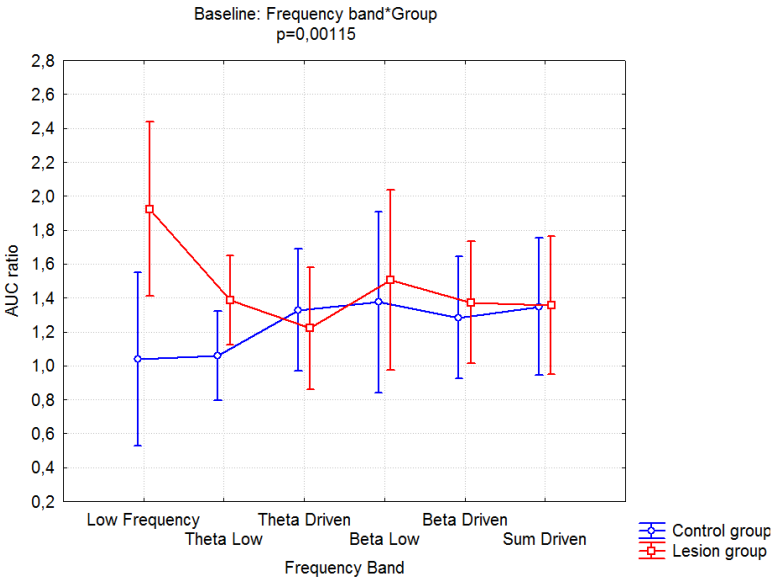

Figure 11. 'Frequency Band*Group' interaction for the baseline. Both graphs are similar, except for the strong "Low Frequency" range. In the lesion group this component significantly differs from the Theta Driven band. (Unweighted Means, Vertical bars denote 0,95 confidence intervals)

Next, we focused on fragments of 'indifferent baseline', taken from the recording before any driving was tested. We hypothesize that the rise in baseline activity we noticed, presumably resulted from the accumulation of stimulation runs. Therefore, we expected to see lower AUC values in all components and no noticeable difference between lesion and control groups. The first assumption appeared to be valid for most cases. Exceptions were found in rats 2212, 0302 and 0702; in some frequency bands, values for the indifferent baseline were slightly higher than the ones obtained in between stimulation sessions. Concerning the second assumption, we -indeed- did not detect any significant differences between the two groups. The p-value for the low frequency component had even risen to 1,0 (MWU, lesion vs control group in low frequency band). Therefore, we normalized all absolute AUC values with this indifferent baseline for all frequency ranges in order to compare them in each rat.

3.2.4.4. **Effect of 'lesion' on driving**

To investigate the effects of intralesional stimulation on the evoked theta, we divided for each frequency band the 'after' by the 'before' AUC value, which were first normalized to the indifferent baseline (Suppl. Table 3). We also included the ratio of the sum of the normalized Theta and Beta Driven, because of the observation that both 10 and 20 Hz components are affected by driving. In a first exploratory approach, we examined if there

was an overall rise of fall in AUC after the 'lesion' by calling four or more ≥ 1 ratio's an "increase", four or more < 1 ratio's a "decrease" and three of each "inconclusive" (Table 4). Applying these criteria to each frequency band revealed that a rising amplitude was the general trend in all considered frequency domains. Moreover, we noticed that almost all "decreases" are situated in the control group, with the exception of rat 2212.

Table 4: Comparison of post- versus pre- 'lesion' AUC values.

Animal	Low Freq	Theta Low	Theta Driven	Beta Low	Beta Driven	Sum
2112	Inconclusive	Increase	Increase	Increase	Inconclusive	Inconclusive
0601	Increase	Increase	Increase	Inconclusive	Inconclusive	Increase
2701	Decrease	Increase	Increase	Increase	Increase	Increase
0102	Increase	Decrease	Inconclusive	Decrease	Decrease	Decrease
0902	Decrease	Increase	Decrease	Decrease	Decrease	Decrease
1502	Increase	Decrease	Increase	Increase	Increase	Increase
2212	Inconclusive	Increase	Decrease	Increase	Decrease	Decrease
2601	Increase	Increase	Inconclusive	Increase	Inconclusive	Inconclusive
0302	Increase	Increase	Increase	Increase	Increase	Increase
0702	Increase	Increase	Increase	Inconclusive	Increase	Increase
1002	Inconclusive	Increase	Increase	Increase	Increase	Increase
1102	Increase	Increase	Increase	Increase	Increase	Increase

Grey boxes denote lesion group

To investigate if there is a significant difference between the two groups across the applied voltages, we ran ANOVA tests for the ratio's per studied frequency band. For "Low Frequency", "Theta Low" or "Beta Low", we found no noticeable trends. The same applied to the driven beta rhythm. "Theta Driven", on the other hand, displayed a p-value of 0,011 for a voltage-difference, though not a group*voltage interaction. Running a post-hoc test, revealed that the discrepancy was located at 6 V, which differed from 9 V (p=0,045) and from 10 V (p=0,015). The accompanying graph, indeed, showed a peak at 6V, followed by a decrease. When separating the two groups, the trends in the plot suggested that the difference was mainly due to the control group, since the lesion group presented with a flatter curve, lacking the prominent 6 V peak (Fig 12 A).
Interestingly, even though "Beta Driven" as such did not produce significant results, the sum of the driven frequency bands had a p-value of 0,014 for a voltage-difference and, additionally, a p-value of 0,031 for the interaction group*voltage. Concerning the voltages, the discrepancy was again situated in 6 V as compared to 8 V (p=0,029), 9 V (p=0,004) and 10 V (p=0,002), once more predominantly due to the 6 V peak in the control group. This maximum is clearly present in the control group of both "Theta Driven" and "Beta Driven" (Fig 12 B,C), implying a mutual contribution. The post-hoc test, however, failed to clarify the group*voltage interaction. Inspecting the accompanying plot (Fig 12 D), revealed a different evolution for control and lesion graphs across the stimulation intensities. AUC ratio's for control rats peaked at 6 V and subsequently dropped until below 1,0. This means that for the highest intensities there appeared to be a decrease in AUC in the 'after' measurements compared to 'before'. The lesioned rats, conversely, did not display this steep fall nor a prominent 6 V peak, but rather maintained a steady level around 1,2. The individual plot of maximum for controls, but then flattens out in both groups around 1,0.

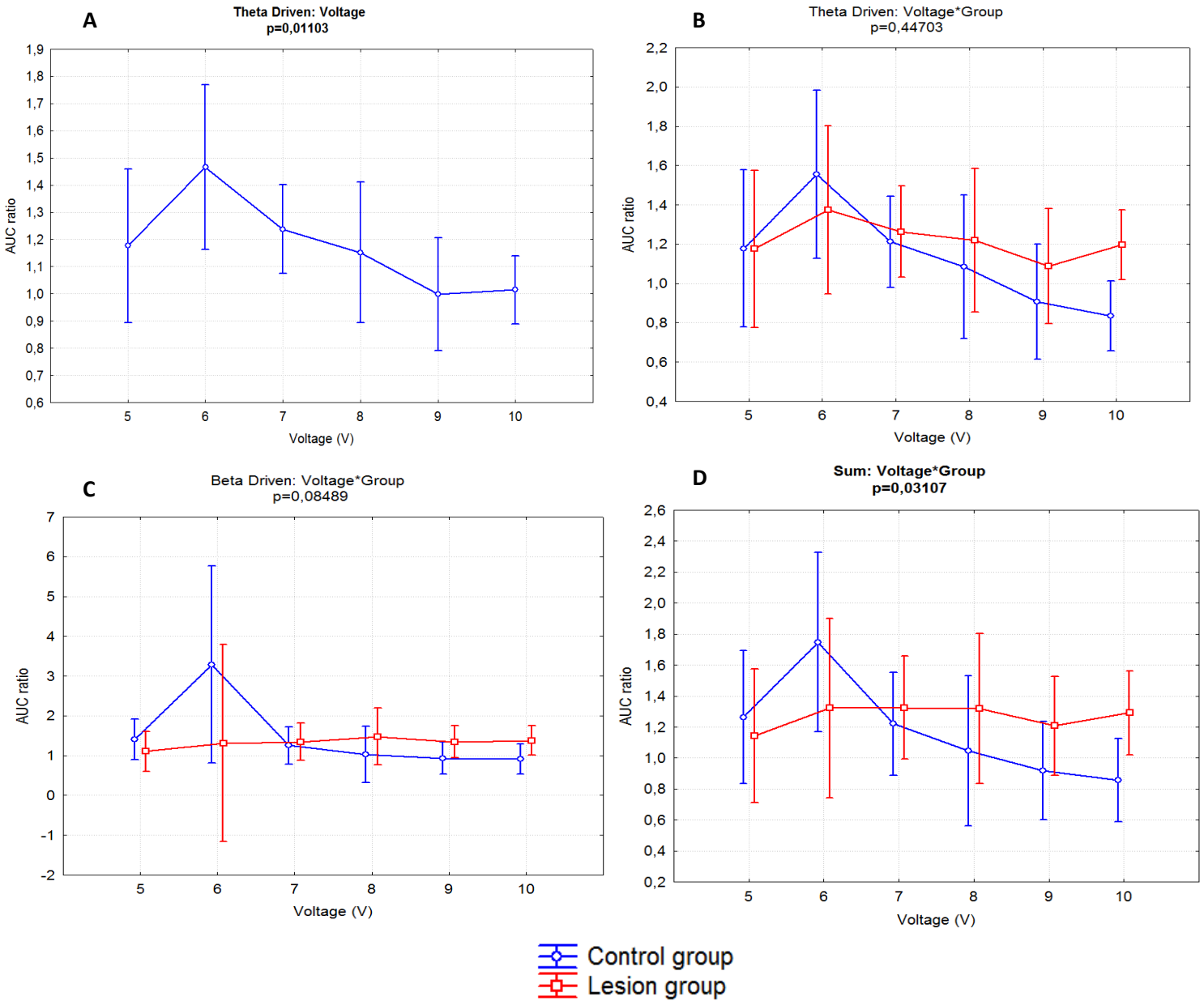

Figure 12. AUC ratio's for different frequency ranges across stimulation intensities.
(A) In the Theta Driven range, a strong enhancement of 6 V AUC values results in a difference with 9 and 10 V. (B) The control group probably contributed the most to this observation, since the 6 V peak is present here, while the curve of the lesion group is much flatter. (C) The 6 V peak is also clear in the control group in the Beta Driven band, suggesting that the contribution to a similar peak in the Sum plot (D) is mutual. This plot shows a different evolution over the voltages in both groups. The control group's AUC ratio peaks at 6 V and then drops to below 1,0, while the lesion group displays a flatter curve. (Unweighted Means. Vertical bars denote 0,95 confidence intervals.)

3.2.5. **Signal averaging**

As described earlier, before the actual large 'theta' peak, we observed a small evoked response. A final step in the data analysis was to identify it by investigating the latency between the electric pulse and the first immediate induction of a reaction. In Matlab, we attempted to calculate the latency between this direct response and the stimulation artifact. The script detects the stimulation artifact and splits the signal in pieces. It then computes the median of the response and searches for peaks and troughs. The final output number is the lag time between the peak of the stimulation artifact and the response. Sometimes multiple values were in the output, indicating that in these cases the response was not equally timed in all pulses. We then included the first value. To keep an honest view, we discarded the animals with more than four out of twelve missing values (N=3). For the animals with a full set (N=4) or missing less than four values (N=5), the lag times were in the same order of magnitude 'before' and 'after' in the same rat, though sporadically an outlying value could occur. The decreases or increases were relatively small and occurred with no obvious difference in lesion or control groups. Additionally, the average latencies were extremely variable across rats and we were unable to identify any trends in the groups. Average lag times ranged from 15 to 55 ms before and from 17 to 51 ms after 'lesion (Table 5).

Table 5: Average latency of evoked response.

Animal	Latency Before (s)	Latency After (s)	# Missing values
2112	0,0466	0,0385	0
0601	*0,0000*	*0,0000*	*7*
2701	0,0503	0,0506	0
0102	*0,0000*	*0,0000*	*7*
0902	0,0291	0,0225	1
1502	0,0551	0,0488	4
2212	0,0431	0,0385	2
0702	0,0451	0,0468	3
1002	0,0308	0,0483	0
0302	0,0153	0,0173	1
2601	0,0279	0,0276	0
1102	*0,0000*	*0,0000*	*11*

Grey boxes denote lesion group
Italique denotes discarded rats

3.3. Discussion

The answer to the question if it is possible to evoke theta rhythm by intralesional stimulation was positive in all cases. As we expected, based on the lesion parameters from literature, our microlesion caused in no animal enough damage to abolish the response. The question as to whether the driving characteristics changed after the intervention is more complicated to address. For a start, it requires a description and/or definition of the observed 'driving'. Due to the variability of the response, this is not a straightforward task.

3.3.1. **The presentation of the elicited waves is highly variable**

A study of theta depictions in literature could shed some light on the (variation in) peak shape we observed. The shown driven rhythm was presented as being a clean, constant and high amplitude response, though only a few seconds are usually published (e.g. (11, 39, 41, 47)). It resembled some stretches of recording we obtained from the rats which we considered to have 'good driving'. A larger wave similarity was seen there as well. Therefore, the variability in peak shape, seems a factor related to quality of driving. Nevertheless, in all figures and our recordings the amplitude is not constant throughout the same stimulation session. Brücke (22) attributes this to the fact that there are still a substantial amount of slow background waves present. We can support this proposition by referring to the multitaper spectrograms. In these, a strong component below 5 Hz is noticeable. In this study, the contribution in this range could be attributed to the use of chloral hydrate as anesthetic. This drug typically presents with EEG activity concentrated in the 0,1 to 3 Hz bandwidth with very little contribution from frequencies higher than 10 Hz for the power spectrum under deep anesthesia. After this period, the distribution becomes bimodal, showing peaks in the 0,1-3 Hz and 5-7 Hz ranges and a small contribution from 10-30 Hz (108, 109). For the lower bandwidths, the peaks in the "Low Frequency" and sometimes "Theta Low" ranges confirm these reports. In the >10 Hz range, we never noticed a peak in the baseline recordings, only a low amplitude background signal. In the stimulation fragments, this signal never came near the driven theta peak, if there was one present.
The variation in polarity of the main peak could partially be explained by slight differences in the electrode position. Since a phase reversal between the two foci of theta activity had been reported before (7, 8, 18, 41, 61), a different location of the recording electrode could be a reason for our observations. Though it needs to be said that an insufficient driving quality sometimes obscures the main response and the polarity.
Looking at one single response, different components could be distinguished. The shape of the wave appeared to be similar for either positive or negative deflections, consistent with the fact that this is not dependent on the layer of recording (22). As has been described in literature (e.g. (26, 80), we also noticed a fast evoked response peak before the actual larger theta peak. This direct reaction to the stimulation can be distinguished from the actual driven waves by shorter rise and, particularly, fall times (26). Consistent with the observations of Williams and Givens (80), the size differed per animal. The authors also found that it always occurred during the first 400 ms after stimulus onset. Our lag time data suggest, however, much shorter reaction times in the first 55 ms. These are closer to the results from the experiments of Brücke et al. (22) in rabbits, who observed latencies as short as 14 ms for the evoked potential.

3.3.2. Electrical stimulation in the MS elicits a high amplitude response of similar waves in the HC time-locked to the pulses

From the vast amount of literature on theta rhythm, we could read at least three characteristics of MS driving. It is a high amplitude response (3) of similar waves (22), which each bear the same fixed relation to the preceding stimulation pulse, therefore having the same frequency (26). In general, visual observations could confirm these features. Although the highest amplitudes in our recordings (circa 0,15 mV, rat 2112) were significantly lower than the maximum of 2 mV Bland et al. (3) propose, in almost all cases the response was visibly higher than the background signal. For the greater part, the waves were in the same rat indeed similar, though not constant throughout the stimulation session, in agreement with Brücke et al. (22). The variety we observed in waveshapes was probably due to a suboptimal driving quality, since rats with good quality theta elicitation also displayed a larger similarity. Finally, if the driving was considered to be 'good', the phase-locking between the theta peak and the stimulation artifact was clearly visible.
Nonetheless, we searched for a more objective measure to confirm that we witnessed driving and not observed a part of the stimulation artifact. We therefore applied EEMD/ICA and broke down the signal in its constitutive sources. Among the most significant components, we isolated a dominant rhythm of approximately 10 Hz in both groups that was absent in baseline fragments. This rhythm corresponded to the prominent peak in the power spectrum and matched the oscillation in the time domain. Moreover, it could always be reconstructed in the presence of stimulation, but not as a part of the stimulation artifact. Thus, this relatively new technique (106) was applied for the first time in theta driving analysis and was able to show that the evoked theta rhythm was not a component of the stimulation, but rather the result of it. Because of these findings, we could interpret the time-varying spectrograms as visualizations of the driven theta. These plots revealed an intense signal in the 10 Hz range at the time of stimulation, which was absent in baseline conditions. Interestingly, at the same moment the harmonic frequencies also showed a higher intensity.

3.3.3. Driving threshold can for the greater part be evaluated by spectral density assessment

According to the driving characteristics of high amplitude, similarity and phase-locking, we qualitatively evaluated the recordings and appointed a driving threshold to each animal. Because of the complexity and subjectivity of this approach, we resorted to signal processing to obtain one objective measure for quality and threshold. We investigated whether spectral density, related to the amplitude factor, is sufficient to give an indication of driving quality. The multitaper spectrograms revealed, besides the low frequency signal, prominent peaks at 10 Hz, 20 Hz and sometimes 30 Hz. These peaks were characteristic for driving, since they were absent in baseline fragments. From these power spectra, we calculated the AUC for five frequency bands, encompassing the range of 1,0 to 22 Hz. Although by using AUC's, the response peak is slightly flattened, it still provides an adequate measure for the amplitude of the signal. For determination of threshold, the sum of "Beta" and "Theta Driven" AUC's was made, resulting from the observation that both these components changed during driving. The derived formula stated that the lowest voltage being 10% higher than the sum of the baseline for these ranges, would be considered the threshold. These results matched the

visual evaluation well. According to our pilot experiments, the minimal threshold to drive a theta rhythm was 4 V, though one study claims intensities as low as 0,5 V were sufficient (42). So, despite the fact that all experimental intensities should be above threshold, some rats showed a >5 V value. Again, this could be a sign of an individual optimal intensity, but in this case it seems more likely to attribute it to low driving quality, probably due to a suboptimal placement of the recording electrode.
Following the hypothesis that higher values above baseline level correspond to better driving, we compared them against the visual evaluation of driving quality. In most cases the highest rated rats also had the highest AUC values, but there were exceptions. For example, rat 0102 presented with a relatively a good visual score, but did not reach the 10% criterion in all voltages. These findings suggest that at least for some animals, other factors should also be taken into account when judging driving quality. Additionally, with aforementioned threshold determination, we assume a linear stimulus-response relationship with better driving at increasing stimulation intensities. However, our observations rather indicate a U-shaped curve with one stimulation optimum per rat. Subsequently, an animal like 1002 could pass the criterion at 5 V, but fail at higher intensities, which raises the question whether it is a fair measure in these cases. Studies have been performed on discovering driving threshold in terms of frequency (26, 29). The authors presented a U-shaped curve with an optimal frequency at 7,7 Hz. In parallel with this observation, we want to propose a similar U-shaped curve for driving intensities. We could, however, not propose one optimum, since it seems to be dependent on the individual animal and/or the position of the recording electrode. It has been reported before that stimulation parameters need to be adjusted for each rat (27, 28), which is consistent with the observed variation. Moreover, suboptimal driving quality could also obscure the optimum and, again, twelve rats might not be sufficient to notice the best driving intensity.

3.3.4. Theta driving at 10 Hz results in a synergetic effect of 10 Hz with its first harmonic 20 Hz

In the stationary and time-varying power spectra, we observed almost every time a second peak at the first harmonic frequency of the driven theta. In some rats, there was even a small 30 Hz signal. The presence of the second peak has been described before and/or is shown in the accompanying figures in many studies (5, 29, 31-39). It is always twice the (driving and evoked) theta frequency, consistent with the signal we see at 20 Hz. Higher harmonics have not been reported in these articles, even though we occasionally spot small peaks at 30 Hz, especially at higher stimulation intensities (e.g. rat 0102, 7 to 10 V, Fig 10 E,F). Some authors describe the second signal as being ‘small’, ‘of low power’ or ‘weak’ (33, 35, 36) or present a figure (5, 39) in which it is clearly subordinate compared to the fundamental. Even when described as ‘clear-cut’ (36), under carbachol and NMDA in urethane-anesthetized rats, it was small. In our findings, however, the 20 Hz peak is usually prominently present, sometimes even overpowering the theta peak (e.g. rat 0102, 6 to 10 V, Fig 10 E,F). The recordings of the animals with strong beta components in the driven rhythm also frequently showed double peaks. On the other hand, it needs to be added that in all but one of the referred literature, theta was evoked pharmacologically with either physostigmine or urethane. Bland et al. (39) applied 10 Hz electrical stimulation and also displayed a weak harmonic signal. It is possible that the used intensity (0,1-0,9 mA) was insufficient to induce a larger beta response. This is at odds with our observation that strong

20 Hz peaks mainly and consistently occur at higher voltages and appear to follow a more linear stimulus-response curve unlike the fundamental. We cannot exclude, though, the possibility that at >10 V stimulation intensities eventually an optimum will appear. Conversely, in parallel with theta, the absolute AUC values of the values normalized to the indifferent baseline vary a great deal. Also in accordance with theta, the threshold for beta occurrence varies among animals and is sometimes not reached, predominantly in the rats with 'bad' driving.

The existence of these harmonic peaks is not surprising, since brain rhythms such as HC theta theoretically resemble the sinusoid pattern of harmonic oscillators (62). Moreover, theta driving can also be elicited by so-called 'gap driving' (26, 29, 30). In this technique a high frequency train of 100 Hz pulses, in itself capable of blocking theta, is presented to the MS, leaving gaps at theta frequencies or harmonics (which produces theta as harmonics). Whether or not the double frequency peaks serve a specific purpose, has not been investigated fully. When examining single neuron responses in rabbits, Vinogradova (37) observed an entrainment effect in a limited frequency range. A resonance tuning of theta cycles was present in the 5 to 10 Hz band, which is typical for a normal alert rabbit. Stimulating with frequencies lower than those of background theta (i.c. 5,5 Hz), entrained rhythmic responses with higher harmonics (e.g. 6 Hz effect during 3 Hz stimulation). Higher frequency stimulation evoked tuning on subharmonics (e.g. 6 Hz effect during 12 Hz stimulation) or escaping of the neuron to its background theta frequency. Since 10 Hz is still within the limits of a rat's theta range, entrainment seems an unlikely explanation for the beta response we observe. As a final point, we could argue that we focused on the evoked theta as being simply the result of external MS driving and ignored the complex interactions which undoubtedly exist in and between both hippocampi. In this view, Gray and McNaughton (29) regarded the phasic MS input as harmonically driving a 'pretuned system', that -in the right conditions- is capable of reinforcing its own oscillations through internal feedback loops. With this in mind, we could propose following model based on our findings. Starting with a baseline lacking any prominent theta or beta peaks, we force a 10 Hz component on it by electrical stimulation of the MS. The rhythmic input of the septum, however, enhances the 20 Hz component as well. Via positive feedback, the enhanced beta component in turn influences the '10 Hz enriched baseline' elicited by stimulation. This loop results in an output of mixed 10 and 20 Hz signals, which are clearly visible as peaks in the power spectra (Fig 13).

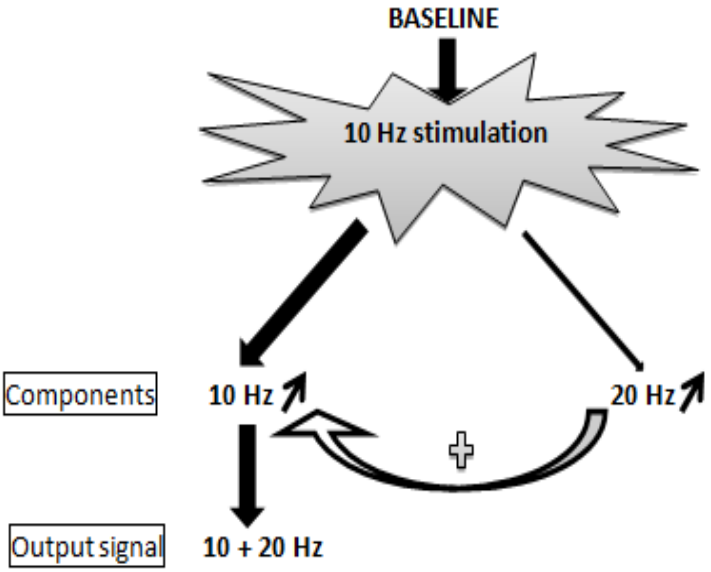

Figure 13. 20 Hz component during stimulation contributes via a feedback loop to the mixed 10+20 Hz output.
A 10 Hz stimulation enhances the 10 Hz component in the baseline. In parallel, it enhances also the 20 Hz, especially with higher stimulation intensities. This second harmonic then influences the '10 Hz enriched' baseline, resulting in a mixed 10+20 Hz response we observe.

3.3.5. **The baseline is influenced over time by increasing stimulation sessions**

Even in the raw recordings, we noticed the baseline becoming more 'restless', 'irritated' over time. With stimulation sessions increasing, it began to display spontaneously more high amplitude peaks. This occured even beyond the direct 'theta-aftereffect' that lasts for few ms after the end of stimulation and is more prominent at higher voltages. Inspecting the power spectra, revealed that it was often the low frequency peak that was enhanced, particularly in the lesion rats. Although the majority of the AUC values indeed rose after the 'lesion' in all frequency bands, never was the difference significant according to the non-parametric tests. However, focusing on the "Low Frequency" band, AUC's in the control group generally seem to be moderately risen over time, while the lesion group's values are more substantially elevated. Rat 2212 was a noticed exception, though it needs to be said that this particular animal showed more atypical results throughout the analysis, including presenting with a relative decrease in driven amplitude after the lesion. Indeed, ANOVA analysis indicated that there was a significant difference in this band compared to the lesion values in the "Theta Driven" band. The plot showed a drop towards the "Theta Driven" range starting from high "Low Frequency" values. The "Beta Driven" range, that is also affected by driving, shows a similar trend. The control group on the other hand revealed a different evolution in the frequency bands. Here, there barely was an enhancement in the "Low Frequency" AUC's, resulting in a lower starting point compared to the lesion group. From the "Theta Driven" range onwards, however, the two plots overlapped. These findings indicate that the distribution of the signal over the studied frequency bands might be slightly different in the two groups, mainly due to the low frequency ranges. We should, however, take into account, that a total of six rats per group is insufficient to build a conclusion on based on the ANOVA results.

3.3.6. **EB reveals damage that extends the visual injury**

In comparison to the lesion parameters reported in literature, ours have a substantially lower intensity. Electrical currents in the range of 1 to 2,5 mA (10, 14, 16, 17, 19, 20, 25) destroyed a large part of the MS and were capable of abolishing theta. The microlesion we induced with a 200 µA current was not sufficient to cause these effects, even with a duration of 15 s. Moreover, the reported lesions were made with stainless steel electrodes, while we used Pt/Ir, a material that generally produces smaller injuries (110). As an additional histological technique, we evaluated EB stained slices to assess BBB permeability. This dye is commonly used as a method for determining blood volume, but can be applied in other cases where damage to the BBB needs to be reviewed as well. EB was taken up by endothelial cells as well as neurons. The fluorescent signal extended further than the visual damage, following the direction of the tract. This directionality suggests it could be caused by mechanical pressure of the insertion. The closest to the electrode trace, the brightest the signal, demonstrating EB kinetics. There was no obvious difference in the MS signal from lesion rats or control rats: both displayed often a rather 'fluffy' injury. On the contrary, HC mechanical lesions -produced by the insertion of the electrode- had more clear-cut edges. This suggests that the fluffiness was typical of an electrical intervention, either by solely stimulating or by both stimulating and lesioning. Indeed, it has been reported before that stimulation itself can be damaging to neural tissue as well (111, 112). Another remarkable

feature we observed was the presence of EB positive granules. Since they were detected in both HC and MS sites, the granules do not seem to be immediately associated with stimulating or lesioning as such. Even though the electrolytic lesion could not be distinguished reliably by this technique, the EB staining still provided additional information about the extent of the damage caused by the entire intervention. Nissl slides were limited by only revealing the visible injury, while the signal on the EB slides clearly extended further. We, therefore, believe this technique to be a valuable addition to damage evaluation.

3.3.7. Lesioned rats show a small trend towards enhanced driving across the applied stimulation intensities

Despite the fact that histological data only showed a minor difference between the two groups, recording analysis did reveal certain changes. In parallel with the baseline observations, AUC values generally increased over time in all frequency domains. Since the few decreases were mostly located in the control group -with the exception of rat 2212- this could be an indication of enhanced driving as evaluated by the response amplitude after a microlesion. We then turned to statistical analysis to verify a potential existence of this trend. In none of the “Low” frequency range, the ANOVA’s could point out a significant difference between the two groups in AUC ratio’s. In the “Driven” bands, we noticed some significant p-values, though not between the groups. First, in the control group a prominent 6 V peak stood out from higher voltages in the “Theta Driven” range as well as in the sum of the “Driven” frequency domains. The same graphical observation was made in the “Beta Driven” band, but remained insignificant. Secondly, regarding the sum, a group*voltage interaction was detected. Control rats followed a similar trend across the voltages in both driven ranges, peaking at 6 V and subsequently dropping to below 1,0, indicating an AUC decrease after the ‘lesion’. Lesion rats, on the other hand, display a different evolution across the voltages, maintaining a steady level in the ‘AUC increase’ region of the plot.
“Beta" and “Theta Driven” plots were quite similar in shape, though the “Beta Driven”-curve had a much larger 6 V peak in controls. The summing of these two frequency domains can be accounted for by the observation that theta and beta are both prominently present in the power spectra as the result of driving. Moreover, it is only when combining these two bands, that the difference in response to the voltages becomes visible. It appears that a decrease in spectral power after the ‘lesion’ is more prominent in the control group, as is the 6 V peak. On the other hand, animals in the lesion group generally appear to maintain an increase, with no apparent optimums (Suppl. Fig 2). At least for the control group, a U-shaped curve is noticeable with a clear optimum at 6 V when considering the sum of Driven bands. This confirms our earlier hypothesis that the stimulus-response curve is not linear. Yet, some remarks have to be kept in mind. First, the variability among the rats is large, which complicates any conclusions. Moreover, it is possible that the preceding baseline could play a role in the presentation of the driven rhythm. We already noticed an influence of driving on the baseline, but to determine the exact extent more research is needed. Finally, as was the case in previous analyses, we must keep in mind that six subjects per group is not enough for making conclusive statements.

3.3.8. **Future directions…**

Because of the complexity of the chosen subject and its results, the analysis can be extended much further. Unfortunately, as the time span to do the research is limited and the analyses often complicated, a part fell outside the scope of this masterthesis. For a start, a chronic variant of the experiment would be helpful to find out whether intralesional stimulation can still work in a gliosis or even in a cavity context. Additionally, the lesion parameters could be adjusted to produce larger lesions and create a stimulus-response curve. Further, whether acute or chronic, more subjects in each group are desirable to achieve more statistical power in the analyses.
Regarding theta research, there is still a need for objective measures of driving quality that include other aspects like phase-locking, aside from amplitude. The same is true when it comes to evaluating the effect of the lesion or establishing threshold values. Another line of research could concern the effects of the baseline in between stimulation sessions on the driven rhythm. Likewise, the effect of the accumulation of stimulation runs on the baseline could be investigated further. Finally, the observed strong 20 Hz component (and higher harmonics) certainly requires additional experiments and analysis.

4. Conclusion

Before starting this research, we asked ourselves two questions. First, is it possible to cause an effect by stimulating in a microlesion and, if yes, how does that effect present itself? Second, is the proposed model valid as a model for lesion restoration? To address these questions, we made use of a 3 to 12 Hz HC oscillation: the theta-rhythm. Advantage has been taken of the fact that it can be elicited by stimulation in the MS and abolished or diminished by lesioning in that location. Studies so far concentrated on either one of these two interventions or targeted different brain areas. In this masterthesis, we attempted to stimulate *and* lesion in the same location in the MS. The microlesions appeared slightly bigger on Nissl than in the control group and in all slices EB staining revealed the larger extent of injured tissue beyond the electrode tract. Despite this damage, it was still possible to evoke an effect by intralesional stimulation. In what aspect driving theta rhythm in the lesion group differed from the control group is a question more difficult to answer.
Visual inspection of the recordings revealed a large variability in all driving characteristics: amplitude, phase-locking and similar waves. To deal with this complexity and find one objective measure to evaluate the effect, we therefore applied signal processing techniques. First, we proved that the observed driving effect was indeed the result of stimulation rather than being a part of the stimulation artifact. Using EEMD/ICA we isolated a 10 Hz dominant rhythm and reconstructed it successfully in the presence of stimulation. Reconstructing the artifact in the same manner, showed that it was only influential in the >50 Hz region. Next, multitaper spectral analysis demonstrated that driving not only enhanced the stimulation frequency, but also its first harmonic -20 Hz- which gained importance towards the higher voltages. This observation also formed the base for the formula we proposed to determine driving threshold objectively. Applying this formula, revealed that a stimulus-response curve for driving was possibly U-shaped instead of linear, with an optimal stimulation intensity. Finally, in order to investigate the effect of the intralesional stimulation on driving, we used AUC values as a measure. We first found that there was a slightly different distribution of the signal over the frequencies 1 to 22 Hz in both groups. This appeared to be mainly due to the

"Low Frequency" range, in which the spectral power was enhanced in the lesion group after the induction of a lesion. Regarding the stimulation, we observed again a slightly different evolution between the groups with respect to the applied voltages. In this case, the importance of both 10 and 20 Hz contributions to driving is emphasized by inspecting the results for the sum values. Control groups show an optimum at 6 V and then a rapid AUC decline towards the higher intensities. Lesion rats on the other hand maintained increased post-lesion values, without apparent optima.
Although our findings suggest a small difference between intralesional and control stimulation, we want to stress that larger groups are necessary to draw such conclusions. As for the question if the proposed model for lesion restoration is valid, the answer is possibly positive. However, a further validation with more animals and in a chronic setting is still required. Whether significant or not, the results still confirm that it is interesting to investigate intralesional stimulation and its effects further.

5. Nederlandse samenvatting

5.1. Inleiding

Eén van de meest prominente lokale veldpotentiaal (LFP) patronen die in de hippocampus (HC) kan geregistreerd worden, is een 3 tot 12 Hz ritmische trage activiteit met de naam 'theta ritme'. Deze sinusachtige oscillatie met amplitudes tot zelfs 2 mV gaat hand in hand met vrijwillige bewegingen zoals stappen of springen, REM-slaap ('type 1 theta' of 'atropine-resistente theta') en is aanwezig onder urethaan of ether anesthesie en sommige vormen van beweegloosheid ('type 2 theta' of 'atropine-gevoelige theta') (3, 4). Het theta ritme is wellicht afkomstig uit hersenstam structuren onder de vorm van niet ritmische ontladingen. Tijdens het opstijgen naar de HC, via de supramammillaire kern (SuM), de posterieure hypothalamische kern (PH) en het mediale septum (MS), nemen deze signalen geleidelijk de juiste frequentie en amplitude aan (3, 5, 6). De amplitude en fase van het geregistreerde ritme hangen kritisch af van de exacte positie van de electrodes in de HC. Daarbij worden de hoogste pieken teruggevonden in Stratum Moleculare en Stratum Oriens; twee lagen die een faseverschil van 180° ten opzichte van elkaar vertonen (7-11).
Al vanaf de eerste experimenten uit de jaren '50 was het duidelijk dat het MS een cruciale rol speelde in theta generatie en behoud (12-14). Elektrolytische letsels op deze plaats -maar niet enkel in het laterale septum, de diagonale band van Broca (DBB) of de mediale regio van het fimbria/fornix (FF) systeem- zijn in staat om een amplitude vermindering of volledige vernietiging van HC theta ritme teweeg te brengen (6, 10, 14-25). Voor een volledige eliminatie lijkt echter uitgebreide schade van het MS noodzakelijk te zijn (16, 20). De letsels die het ritme enkel verstoren zijn kleiner, maar waren altijd gelokaliseerd in het MS en liepen vaak verder door tot in de DBB (16).
Bovendien blijkt de sterke septo-hippocampale band ook duidelijk uit het '*driving'* fenomeen (12, 26-28). Laagfrequente elektrische MS stimulatie binnen het theta bereik is in staat een theta ritme op te wekken in de HC, waarvan de fase vastgezet is op de stimulatie pulsen ('*phase-locking'*). Naast *phase-locking* wordt theta ook gekenmerkt door amplitudeverhoging en het uitzicht van gelijkaardige golven. Hoewel hoog-frequente stimulatie het ritme kan blokkeren, kan het toch *driving* induceren wanneer gaten gelaten worden op theta-frequenties of gehele meervouden hiervan (26, 29, 30). Het resulterende *power* spectrum vertoont doorgaans een piek bij de stimulatiefrequentie en de eerste

harmonische frequentie (5, 29, 31-39). De *driving* intensiteiten vermeld in vorige studies variëren van 0,5 tot 10 V and van 1 tot 900 µA en zijn afhankelijk van het dier (22, 26-28, 39-42). Wat betreft de stimulatiefrequentie, gelden voor elk dier eveneens individuele drempel parameters, maar traditioneel wordt 7,7 Hz voorgesteld (26). Het *driving* effect is zichtbaar tot ongeveer 30 Hz, hoewel Wetzel (42) meende dat stimulatie met frequenties hoger dan theta, resulteerde in theta frequenties.
Het opgewekte theta ritme gelijkt sterk op het fysiologische ritme, wat betreft frequentie, golfvorm, amplitude en fase diepteprofielen (22, 28, 41, 42). De stimulatie veroorzaakt ook acetylcholine (ACh) vrijzetting in de HC (43) en bootst de respons op atropine en urethaan na op dezelfde wijze als het natuurlijke theta ritme, wat impliceert dat type 1 en 2 eveneens op deze manier kunnen onderscheiden worden (28). In vrij-bewegende dieren, echter, is het opgewekte theta ritme gedissocieerd van normale gedragscorrelaties. Daarom werd geopperd dat elektrische stimulatie van het MS inderdaad het theta-genererende circuit kan activeren, maar op een niet-fysiologische manier. Een substantieel deel van het onderzoek naar dit ritme werd utgevoerd in ratten en konijnen, hoewel ook dieren als katten, cavia's of muizen gebruikt worden (voor een discussie, zie (7, 44)). Waarschijnlijk zijn er geen grote verschillen tussen de soorten, aangezien ze allemaal beide types van theta kunnen produceren. Met de uitzondering van primaten, is in alle onderzochte dieren ook een correlatie met simultaan gedrag aanwezig, maar elke soort zou eventueel een eigen set theta-gerelateerd gedrag bezitten (7, 44).

Het MS is de locatie geweest van ofwel letselinductie ofwel stimulatie om het effect op HC theta te testen. Om post-letsel resultaten te beschrijven, zochten auteurs meestal hun toevlucht tot vrij-bewegende of met urethaan verdoofde dieren, die een spontaan ritme vertonen (10, 21, 45), stimuleerden op een andere hersenregio zoal de PH (46) of implementeerden een bypass circuit (47). Door voordeel te halen uit de feiten dat kleine MS letsels theta kunnen verminderen en MS stimulatie theta kan opwekken, onderzochten we het effect van intralesionale stimulatie op het opgewekte theta en evalueerden het als een adequaat model voor letselrestauratie. Het effect van letselinductie werd voorheen typisch nagegaan aan de hand van amplitude of spectrale power. In de gevallen waar geen volledige vernietiging van theta was verkregen, werd een verlaagde amplitude (bv. (14, 19, 45)) of reductie in spectrale power in het theta-bereik (bv. (47)) gerapporteerd. Om deze reden, werden de vernoemde maatstaven eveneens geïncludeerd in het voorliggende werk om te onderzoeken of intralesionale stimulatie een potentiële vermindering in amplitude kan opvangen.

5.2. Experimenteel design

Daartoe werden 12 mannelijke Wistar ratten paarsgewijs at random ingedeeld in twee groepen: een letselgroep (N=6) en een controlegroep (N=6). Bij alle dieren werden na verdoving (Chloral Hydraat 0,5 g/kg) twee bipolaire Pt/Ir electrodes ingebracht: met volgende coördinaten volgens Paxinos' en Watson's stereotactische atlas (1): AP 0,5 mm, ML 1,2 mm, SD 6,2 mm voor de stimulatie/letsel electrode (MS regio) en AP -3,3 mm, ML 2,2, SD 2,6 mm voor de recording electrode (HC regio). LFP's werden continu geregistreerd ter hoogte van de HC met behulp van een 1-kanaals head-stage versterker (AM Systems, model 3000). Het signaal werd gefilterd tussen 0,1 Hz en 3,0 kHz (band-stop filter 50 Hz), 500 maal versterkt en gedigitaliseerd met een mk1401 CED-eenheid aan 10 kHz. Volt-gecontroleerde

elektrische stimulatie (pulsbreedte 1,0 ms) werd toegepast in het MS met intensiteiten variërende tussen 5 en 10 V en bij een 10 Hz frequentie. Een elektrolytisch letsel werd via dezelfde elektrode geïnduceerd door de passage van een 200 µA DC stroom voor 15 s met behulp van een WPI DS8000 stimulatie isolatie-eenheid. De optimale *driving*- en letsel parameters werden eerder vastgesteld in een reeks pilootexperimenten (N = 10). Bij het beoordelen van *driving*, werden drie kenmerken van de grootste responspiek (d.i. de theta-piek) geëvalueerd: de *phase*- of *time-locking* aan het stimulatie artefact, de toename in amplitude en gelijkaardigheid van de golven. In geen geval was 4 V genoeg om *driving* te induceren. De beste stimulatie frequentie om theta in de HC uit te lokken, bleek 10 Hz te zijn, hoewel het *driving* effect kon bekomen worden in een bereik van 8 tot 30 Hz. Met de bedoeling om grootschalige vernieling van het MS te vermijden, werden deze letselparameters gekozen die de laagste intensiteit (200 µA) en duur (15 s) hadden, maar nog steeds weefselschade teweegbrachten.
Na correcte plaatsing van de elektroden, werd een stimulatie testpuls van 1 Hz aan 1 V gegeven, terwijl het optreden van het artefact werd gecontroleerd op het scherm. Vervolgens werd een *driving* puls van 10 Hz aan 5 V toegediend en het uitlokken van een reactie werd visueel bevestigd. Een pre-'letsel' recording van theta-*driving* werd daarna in alle ratten geregistreerd. Deze bestond uit een serie van zes stimulatie sequenties, gescheiden door een 3 min durende stimulatie-OFF periode. Elke run werd gekenmerkt door een andere stimulatie-intensiteit, willekeurig toegewezen uit de waarden 5, 6, 7, 8, 9 en 10 V, met een vaste frequentie van 10 Hz en duur van 6 s. Nadien werd enkel bij de experimentele groep een elektrolytisch letsel in de MS toegebracht (200 µA, 15 s). Voor de post-'letsel' recording werden beide groepen opnieuw onderworpen aan hun pre-'letsel' stimulatie sequentie. Na het elektrofysiologisch gedeelte werd i.v. Evans Blue (EB) toegediend en na 15 min werden de dieren ge-euthanaseerd met een CO_2 overdosis en transcardiaal geperfuseerd met 10% sucrose, gevolgd door 4% formaldehyde. Ten slotte werd de positie van de elektroden en de omvang van het letsel histologisch geverifieerd met Nissl (d.i. cresyl violet) kleuring, terwijl Evans Blue (EB) kleurstof aanvullende informatie verstrekte over de schade aan de bloed-hersen barrière (BBB).

5.3. Resultaten en discussie

De presentatie van de thetagolven was in het algemeen erg variabel. We observeerden mono-, bi- en trifasische golven en zowel positieve als negatieve polariteiten. Bovendien werd de eigenlijke theta-golf vaak vooraf gegaan door een snelle, kleinere directe respons. Deze vond meestal plaats binnen de eerste 51 ms na stimulatie, eerder in het bereik van de 14 ms die Brücke (22) rapporteerde voor konijnen dan de tragere 400 ms van Williams en Givens (80). De afbeeldingen van een theta-ritme uit de literatuur toonden typisch een hoge amplitude, zuivere en constante respons. Deze leek op delen van onze recordings van de ratten met 'goede *driving*', wat suggereert dat de factor van variabiliteit samenhangt met de kwaliteit van theta-opwekking. Toch wordt ook vermeld dat de amplitude meestal niet constant is doorheen de stimulatiesessie (22), vanwege de sterke aanwezigheid van trage achtergrondgolven. De multitaper spectrogrammen demonstreerden inderdaad ook een sterke aanwezigheid van de <5 Hz component. Waarschijnlijk is deze bijdrage nog versterkt door het gebruik van chloral hydraat, aangezien de spectrale activiteit van dit anestheticum zich concentreert in de lage frequenties. De observatie van de verschillende polariteiten kan

dan weer te wijten zijn aan de licht verschillende positie van de recording electrode, want faseverschillen tussen HC lagen werden al elders beschreven (7, 8, 18, 41, 61).
Het ritme dat we waarnemen op de recordings is consistent met de eigenschappen toegeschreven aan theta in de literatuur: hoge amplitude (3), gelijkaardige golven (22) en zelfde frequentie als de stimulatie ten gevolge van *phase-locking* (26). Afwijkingen hiervan zijn waarschijnlijk te wijten aan een suboptimale *driving*-kwaliteit. Met behulp van EEMD/ICA hebben we het volledige signaal opgedeeld in de afzonderlijke 'bronnen' dat het bevat. In die 'bronnen', hebben we een dominant ritme van ongeveer 10 Hz kunnen isoleren dat overeenkwam met de grootste piek in het power spectrum en de oscillatie in het tijdsdomein. Het was daarentegen afwezig in de baselinefragmenten. Bovendien konden we met eenzelfde techniek aantonen dat het 10 Hz ritme geen deel uitmaakte van het stimulatieartefact, maar er eerder een gevolg van was.
Volgens de bovenbeschreven karakteristieken beoordeelden we de recordings op *driving*-kwaliteit en identificeerden een *driving*-drempel per dier. Om deze observaties objectief te bevestigen, werden multitaper-spectrogrammen gemaakt, waarbij spectrale densiteit gezien werd als een maat voor de factor 'amplitude'. De bekomen spectra vertoonden typisch prominente pieken op 10, 20 en soms 30 Hz voor de stimulatiefragmenten. Daarna berekenden we de bijhorende AUC voor vijf frequentiebanden: "Low Frequency" (1,0-4,80 Hz), "Theta Low" (4,81-8,18 Hz), "Theta Driven" (8,19-11,82 Hz), "Beta Low" (11,83-17,99 Hz) and "Beta Driven" (18,0-22,0 Hz). Rekening houdend met de consistente aanwezigheid van zowel theta als de eerste harmonische beta (20 Hz) piek, maakten we de som van beide AUC waarden. De vervolgens afgeleide formule stelt dat de laagste intensiteit, die 10% hoger is dan de gesommeerde baseline theta en beta AUC-waarden, beschouwd wordt als *driving*-drempel. De zo verworven waarden waren gelijkaardig aan degene bekomen met de visuele observatie, wat suggereert dat amplitude voor een groot deel de *driving*-drempel kan identificeren. Aan de andere kant, vaak hebben hogere voltages toch AUC-waarden die lager liggen dan de drempel. Dat doet vermoeden dat de stimulus-respons curve eerder U-vormig dan lineair is.
Hoewel de stimulatie gebeurde met 10 Hz , is de sterke 20 Hz piek prominent aanwezig in zowel de stationaire als in tijd variërende power spectra, zeker aan hogere voltages. De aanwezigheid van harmonische pieken na stimulatie werd reeds eerder vermeld (5, 29, 31-39), hoewel steeds beschreven als 'zwak'. Ze zouden afkomstig kunnen zijn van interne feedback loops in de HC (29). Met dit in het achterhoofd, stellen we daarom hetvolgende model voor. Aan een baseline zonder enige opvallende theta of beta pieken hebben we eerst door middel van elektrische stimulatie van het MS een 10 Hz component opgedrongen. De ritmische septale input vergrootte echter gelijktijdig de 20 Hz bijdrage. Via positieve feedback heeft deze vergrote beta-component dan op zijn beurt invloed op de 'met 10 Hz verrijkte baseline' uitgelokt door stimulatie. Deze lus resulteert dan ten slotte in de gemengde 10 en 20 Hz signalen die we observeren als pieken in de power spectra.
In het voorgaande is er nooit een significant verschil gezien tussen letsel en controlegroep. Dit kan te wijten zijn aan het feit dat het letsel zelf erg klein was. Op de Nissl gekleurde coupes was slechts een beperkt grootteverschil zichtbaar. Om het letsel verder te karakteriseren, gebruikten we de EB kleurstof, die bindt aan albumine en een indicator is voor BBB schade. Zowel beschadigde neuronen als endotheelcellen rond de bloedvaten reageerden positief. Het fluorescentiesignaal reikte verder dan het eigenlijke elektrode letsel en vertoonde een zekere directionaliteit in het verlengde van het elektrodespoor. De MS letsels vertoonden vaak meer 'pluizige' randen, terwijl deze in de HC scherper afgelijnd

waren. Het ‘pluizige’ uiterlijk houdt waarschijnlijk verband met een elektrische interventie (stimulatie of elektrolytisch letsel). Een andere observatie is tot slot de aanwezigheid van EB-positieve granulen in de beschadigde neuronen van zowel HC als MS.
Hoewel het om een microletsel gaat, is er toch enige invloed merkbaar op de HC ritmes wanneer we op deze locatie stimuleren. In eerste instantie komt dit effect tot uiting in de baseline. De visuele inspectie onthulde al een meer ‘geïrriteerde’ achtergrondactiviteit met hogere en snellere pieken, naarmate meer stimulatiesessies elkaar opvolgden. Dit werd bevestigd door een ANOVA-analyse op de AUC ratio’s, beschouwd over het bestudeerde frequentiebereik. Hieruit bleek dat in de eerste plaats de amplitude in alle ratten gestegen was, maar dat in de lage frequenties een verschil zat in de interactie frequentieband*groep ($p=0,001$). In de letselgroep de 1 tot 4,8 Hz component is duidelijk sterker gestegen en zakt dan naar de “Theta Driven” waardes. Anderzijds beginnen de waardes voor dit bereik in de controlegroep lager, maar bereiken hetzelfde punt op “Theta Driven”. In de stimulatiewaarden is er eveneens een ander verloop merkbaar van de curves voor letsel en controlegroep. Zowel voor het opgewekte theta als beta is er in de controlegroep een sterke 6 V piek te vinden, die vervolgens overgaat in een daling van AUC-ratio’s bij de hogere voltages. De letselgroep daarentegen vertoont een vlakker verloop en blijft steeds boven de drempel om van een stijging te spreken (=1). De voltage*groep interactie suggereert dat bij intralesionale stimulatie beide groepen een andere evolutie vertonen over het verloop van stijgende stimulatie-intensiteiten, waarbij de letselgroep een mogelijk verbeterde *driving* kan hebben in de hoogste voltages, gemeten als amplitudestijging.

5.4. Besluit

In alle ratten kon er na het ‘letsel’ nog een ritme opgewekt worden. De stimulatiefragmenten vertoonden variabele pieken, die een sterke 10 en 20 Hz component bevatten. De drempel voor *driving* werd daarom bepaald aan de hand van een afgeleide formule waarin ook deze beta-bijdrage inbegrepen was. De baseline verhoogde gemiddeld in amplitude voor beide groepen, maar in de lage frequenties, verschilde ze van de letselgroep. Het letsel zelf bleek klein te zijn en werd ook gekarakteriseerd met behulp van EB. Op deze manier werd de uitgebreidere schade aan de BBB zichtbaar. Deze techniek is dus zeker een waardevolle aanvulling op de Nissl-kleuring die enkel de zichtbare schade van het elektrodespoor toont.
Ondanks het feit dat we nergens een groepseffect konden aantonen, vonden we toch een significante interactie over de stimulatie-intensiteiten heen. Het verloop van de letselgroep geeft een aangehouden amplitudestijging aan in beta en theta banden, terwijl deze in de controlegroep piekt op 6 V en dan verder daalt. Omwille van deze observatie, kunnen we suggereren dat het voorgestelde model voor letselrestauratie een mogelijke validiteit heeft. Toch moet daarbij steeds in het achterhoofd gehouden worden dat een groep van zes ratten onvoldoende is om besluiten uit te trekken. Voor een sterkere validatie van het model zou het daarom ook getest moeten worden in een chronische situatie en met meer proefdieren per groep.

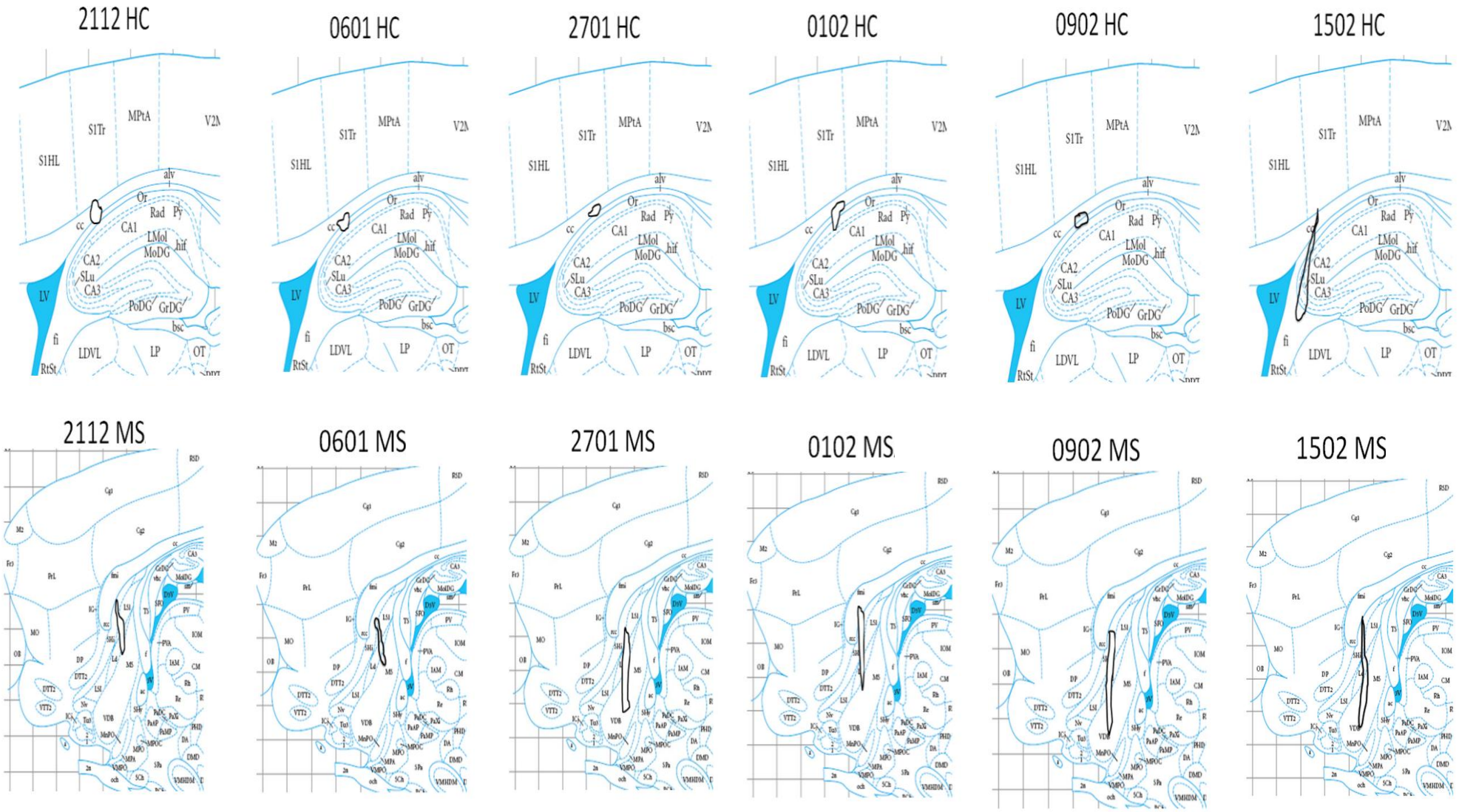

Supplementary Figure 1

Supplementary Figure 1. Electrode positions on stereotactic atlas by Paxinos and Watson (1): control group.
The lesions caused by insertion of the electrode were verified on the Nissl slices. The slice which showed the electrode tip is represented in these drawings, including -when visible- part of the tract. See also Table 1. Figures are adapted from (1) with lateral coordinate of 0,18 mm.

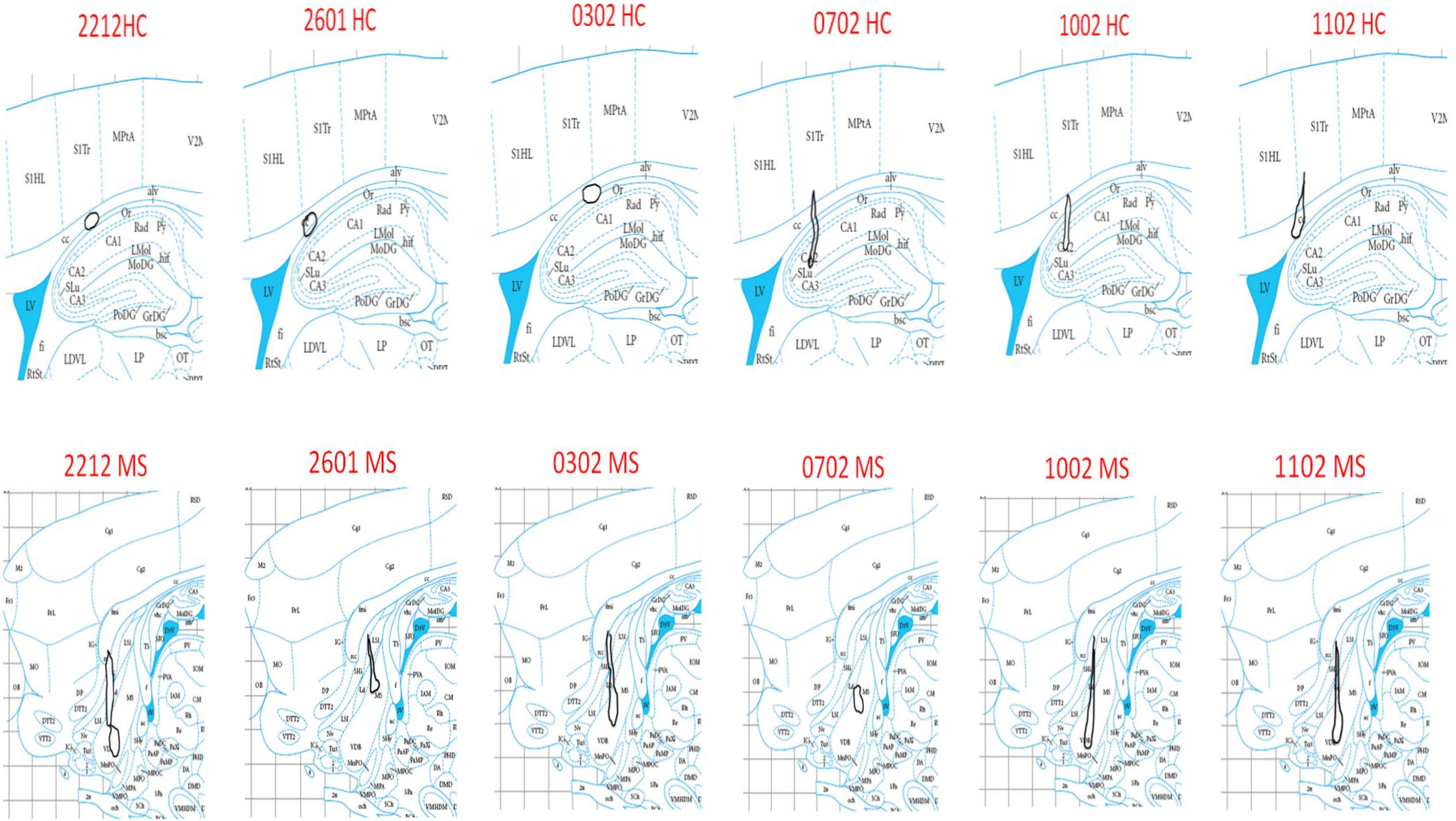

Supplementary Figure 1

Supplementary Figure 1. Electrode positions on stereotactic atlas by Paxinos and Watson (1): lesion group.
The insertion and electrolytic lesions were verified on the Nissl slices. The slice which showed the electrode tip is represented in these drawings, including -when visible- part of the tract. See also Table 1. Figures are adapted from (1) with lateral coordinate of 2,40 mm. See also table 1.

Supplementary Figure 2

ABSTRACT:

Signal analysis of the effects of microlesions in the medial septal area on the dominant hippocampal rhythm in anesthetized rats

K Mols[1,2], I Gligorijevic[3], D. Prodanov[1,2], B Nuttin[2]

1)Bioelectronic Systems group, IMEC, Leuven, Belgium; 2) Laboratory of Experimental Functional Neurosurgery, Katholieke Universiteit Leuven (KU Leuven), Leuven, Belgium; 3) ESAT, KU Leuven, Leuven, Belgium

The theta-rhythm in the rat has been implicated in attention, motivation, learning and memory. The aim of the present experiment was to establish whether electrical stimulation in the acutely lesioned medial septal area (MSA) could have an effect on the hippocampal rhythm in anesthetized animals. Adult male Wistar rats (n=6) were anesthetized with 0.5 g/kg chloral hydrate. Two Pt bipolar twisted pair electrodes were implanted in MSA (AP 0.5 ML 1.2 SD 6.2 mm 10°) and the hippocampus (AP -3.3 ML 2.2 SD 2.6 mm 10°). Local field potentials (LFPs) were recorded in the band 0.1 Hz - 3k Hz and digitized at 10 kHz using *Spike2* (CED). Voltage-controlled stimulation (pulse width 1 ms) in the MSA site was performed in the range of 5 – 10V at frequencies between 4 and 50 Hz. Electrolytic lesions were made by 200 uA DC current for 15 s. Post lesion stimulation was performed with the same protocol. The stimulation in MSA in the range 10 – 25 Hz was able to elicit time-locked rhythm in the hippocampus (i.e. rhythm driving). The threshold for driving was 5.18 V. The LFPs were analyzed with the Chronux package (1); and Ensemble Empirical Mode Decomposition/ Independent Component Analysis (EEMD-ICA) (2). The driving was characterized by marked peaks in the multi-taper spectrum around 10, 20 and 30 Hz. EEMD-ICA could objectively isolate the driven rhythm and reconstruct it successfully in the presence of stimulation. Components characteristic of driving were observed only during stimulation and were not part of the stimulation artifact (reconstructed by the same procedure). Preliminary results demonstrate that at the driving threshold, in 4 cases the lesions increased the component at 10 Hz, in 1 case had no effect and in 1 case there was no appreciable difference between pre and post-lesion state.

References

1.Mitra P. and H. Bokil (2008). Observed Brain Dynamics. Oxford University Press
2.Mijovic B., De Vos M., Gligorijevic I., Taelman J., Van Huffel S. (2010). *IEEE Trans Biomed Eng*, 57(9), 2188 – 2196

Suppl. Figure 2. Abstract for SAN meeting.
The abstract based on this thesis was accepted for the meeting of the Society of Applied Neurosciences in Thesssaloniki and will be presented there between May 5 and 8 2011.

Supplementary Table 1

Suppl. Table 1: AUC values for threshold determination.

		Theta Driven: 8,19-11,82 Hz		Beta Driven: 18-22 Hz		Theta + Beta	
Animal	**V**	**Before**	**After**	**Before**	**After**	**Sum Before**	**Sum After**
2112	*5*	0,0138	0,0257	0,0084	0,0138	0,0222	0,0395
	6	0,0144	0,0256	0,0100	0,0108	0,0244	0,0364
	7	0,0193	0,0190	0,0125	0,0119	0,0318	0,0309
	8	0,0202	0,0164	0,0117	0,0135	0,0319	0,0299
	9	0,0160	0,0188	0,0128	0,0119	0,0288	0,0307
	10	0,0160	0,0164	0,0132	0,0121	0,0292	0,0285
	Base	**0,0062**	**0,0131**	**0,0048**	**0,0087**	**0,0110**	**0,0218**
0601	*5*	0,0051	0,0091	0,0020	0,0043	0,0071	0,0134
	6	0,0071	0,0098	0,0023	0,0048	0,0094	0,0146
	7	0,0073	0,0091	0,0032	0,0047	0,0105	0,0138
	8	0,0096	0,0104	0,0072	0,0051	0,0168	0,0155
	9	0,0082	0,0094	0,0042	0,0040	0,0124	0,0134
	10	0,0140	0,0085	0,0084	0,0059	0,0224	0,0144
	Base	**0,0023**	**0,0038**	**0,0014**	**0,0025**	**0,0037**	**0,0063**
2701	5	0,0066	0,0066	0,0029	0,0051	0,0095	0,0117
	6	0,0038	0,0079	0,0018	0,0057	0,0056	0,0136
	7	0,0042	0,0070	0,0025	0,0045	0,0067	0,0115
	8	0,0061	0,0061	0,0030	0,0033	0,0091	0,0094
	9	0,0092	0,0046	0,0047	0,0033	0,0139	*0,0079
	10	0,0097	0,0071	0,0046	0,0052	0,0143	0,0123
	Base	**0,0025**	**0,0035**	**0,0025**	**0,0038**	**0,0050**	**0,0073**
0102	5	0,0151	0,0086	0,0118	0,0085	0,0269	*0,0171
	6	0,0090	0,0191	0,0102	0,0126	*0,0192	0,0317
	7	0,0107	0,0150	0,0118	0,0110	0,0225	0,0260
	8	0,0107	0,0119	0,0126	0,0101	0,0233	0,0220
	9	0,0153	0,0052	0,0152	0,0095	0,0305	*0,0147
	10	0,0136	0,0122	0,0148	0,0124	0,0284	0,0246
	Base	**0,0104**	**0,0107**	**0,0085**	**0,0090**	**0,0189**	**0,0197**
0902	5	0,0034	0,0029	0,0028	0,0024	*0,0062	*0,0053
	6	0,0031	0,0022	0,0025	0,0018	*0,0056	*0,0040
	7	0,0028	0,0026	0,0032	0,0023	*0,0060	*0,0049
	8	0,0037	0,0026	0,0030	0,0022	*0,0067	*0,0048
	9	0,0029	0,0030	0,0028	0,0024	*0,0057	*0,0054
	10	0,0030	0,0027	0,0031	0,0026	*0,0061	*0,0053
	Base	**0,0038**	**0,0028**	**0,0026**	**0,0025**	**0,0064**	**0,0053**
1502	5	0,0025	0,0025	0,0023	0,0030	0,0048	0,0055
	6	0,0023	0,0029	0,0015	0,0026	*0,0038	0,0055

	7	0,0023	0,0024	0,0022	0,0036	*0,0045	0,006
	8	0,0020	0,0036	0,0015	0,0025	*0,0035	0,0061
	9	0,0032	0,0040	0,0018	0,0028	0,0050	0,0068
	10	0,0037	0,0031	0,0024	0,0025	0,0061	0,0056
	Base	**0,0024**	**0,0025**	**0,0018**	**0,0020**	**0,0042**	**0,0045**
2212	*5*	0,0099	0,0090	0,0078	0,0046	0,0177	0,0136
	6	0,0097	0,0092	0,0075	0,0048	0,0172	0,0140
	7	0,0117	0,0140	0,0078	0,0051	0,0195	0,0191
	8	0,0095	0,0080	0,0085	0,0057	0,0180	0,0137
	9	0,0098	0,0096	0,0098	0,0074	0,0196	0,0170
	10	0,0082	0,0083	0,0083	0,0072	0,0165	0,0155
	Base	**0,0055**	**0,0048**	**0,0065**	**0,0050**	**0,0120**	**0,0098**
2601	5	0,0060	0,0051	0,0057	0,0032	0,0117	*0,0083
	6	0,0049	0,0054	0,0053	0,0042	0,0102	0,0096
	7	0,0070	0,0066	0,0041	0,0050	0,0111	0,0116
	8	0,0053	0,0067	0,0045	0,0047	0,0098	0,0114
	9	0,0076	0,0064	0,0051	0,0042	0,0127	0,0106
	10	0,0079	0,0083	0,0037	0,0049	0,0116	0,0132
	Base	**0,0035**	**0,0049**	**0,0039**	**0,0032**	**0,0074**	**0,0081**
0302	5	0,0013	0,0023	0,0011	0,0022	*0,0024	*0,0045
	6	0,0013	0,0025	0,0011	0,0028	*0,0024	0,0053
	7	0,0013	0,0021	0,0013	0,0031	0,0026	0,0052
	8	0,0015	0,0025	0,0014	0,0030	0,0029	0,0055
	9	0,0024	0,0029	0,0016	0,0028	0,0040	0,0057
	10	0,0021	0,0033	0,0017	0,0042	0,0038	0,0075
	Base	**0,0013**	**0,0018**	**0,0010**	**0,0028**	**0,0023**	**0,0046**
0702	5	0,0093	0,0122	0,0073	0,0111	0,0166	0,0233
	6	0,0084	0,0137	0,0103	0,0079	0,0187	0,0216
	7	0,0097	0,0117	0,0073	0,0102	0,0170	0,0219
	8	0,0100	0,0078	0,0092	0,0066	0,0192	0,0144
	9	0,0115	0,0131	0,0093	0,0140	0,0208	0,0271
	10	0,0120	0,0155	0,0102	0,0135	0,0222	0,029
	Base	**0,0052**	**0,0049**	**0,0035**	**0,0057**	**0,0087**	**0,0106**
1002	5	0,0048	0,0053	0,0037	0,0035	0,0085	0,0088
	6	0,0035	0,0038	0,0032	0,0043	0,0067	*0,0081
	7	0,0035	0,0048	0,0032	0,0036	0,0067	*0,0084
	8	0,0037	0,0037	0,0031	0,0031	0,0068	*0,0068
	9	0,0042	0,0037	0,0033	0,0038	0,0075	*0,0075
	10	0,0043	0,0041	0,0033	0,0038	0,0076	*0,0079
	Base	**0,0032**	**0,0041**	**0,0025**	**0,0038**	**0,0057**	**0,0079**
1102	5	0,0045	0,0050	0,0016	0,0016	0,0061	0,0066
	6	0,0043	0,0067	0,0014	0,0025	0,0057	0,0092
	7	0,0040	0,0050	0,0013	0,0017	0,0053	0,0067

	8	0,0033	0,0058	0,0010	0,0033	0,0043	0,0091
	9	0,0033	0,0049	0,0011	0,0023	0,0044	0,0072
	10	0,0040	0,0052	0,0021	0,0024	0,0061	0,0076
	Base	**0,0020**	**0,0029**	**0,0012**	**0,0018**	**0,0032**	**0,0047**

Grey boxes denote lesion group

(*) denotes below threshold, defined as <10% of baseline sum (theta+beta)

Supplementary Table 2

Suppl. Table 2. Baseline AUC values and ratio.

	Low freq 1,0-4,8Hz			Theta Low: 4,8-8,18Hz			Theta Driven: 8,19-11,82Hz		
Animal	Before	After	Ratio	Before	After	Ratio	Before	After	Ratio
2112	0,0150	0,0126	*0,8400	0,0073	0,0113	1,5479	0,0062	0,0131	2,1129
0601	0,0076	0,0074	*0,9737	0,0036	0,0036	1,0000	0,0023	0,0038	1,6522
2701	0,0049	0,0062	1,2653	0,0034	0,0025	*0,7353	0,0025	0,0035	1,4000
0102	0,0277	0,0291	1,0505	0,0108	0,0109	1,0093	0,0104	0,0107	1,0288
0902	0,0051	0,0059	1,1569	0,0030	0,0033	1,1000	0,0038	0,0028	*0,7368
1502	0,0060	0,0057	*0,9500	0,0026	0,0025	*0,9615	0,0024	0,0025	1,0417
2212	0,0087	0,0073	*0,8391	0,0050	0,0050	1,0000	0,0055	0,0048	*0,8727
2601	0,0078	0,0150	1,9231	0,0065	0,0082	1,2615	0,0035	0,0049	1,4000
0302	0,0016	0,0051	3,1875	0,0012	0,0023	1,9167	0,0013	0,0018	1,3846
0702	0,0093	0,0170	1,8280	0,0049	0,0065	1,3265	0,0052	0,0049	*0,9423
1002	0,0056	0,0085	1,5179	0,0031	0,0040	1,2903	0,0032	0,0041	1,2813
1102	0,0036	0,0081	2,2500	0,0025	0,0038	1,5200	0,0020	0,0029	1,4500

	Beta Driven: 18-22Hz			Beta Low: 11,83-17,99Hz			Sum Theta + Beta Driven		
Animal	Before	After	Ratio	Before	After	Ratio	Before	After	Ratio
2112	0,0048	0,0087	1,8125	0,0122	0,0210	0,0067	3,6608	0,0110	0,0030
0601	0,0014	0,0025	1,7857	0,0028	0,0050	0,0016	2,6522	0,0037	0,0014
2701	0,0025	0,0038	1,5200	0,0046	0,0066	0,0030	2,1353	0,0050	0,0023
0102	0,0085	0,0090	1,0588	0,0157	0,0144	0,0148	2,0381	0,0189	0,0093
0902	0,0026	0,0025	*0,9615	0,0065	0,0051	0,0068	1,8368	0,0064	*0,0035
1502	0,0018	0,0020	1,1111	0,0035	0,0037	0,0032	2,0032	0,0042	0,0021
2212	0,0065	0,0050	*0,7692	0,0105	0,0083	0,0137	1,8727	0,0120	*0,0064
2601	0,0039	0,0032	*0,8205	0,0072	0,0079	0,0088	2,6615	0,0074	0,0028
0302	0,0010	0,0028	2,8000	0,0021	0,0038	0,0008	3,3013	0,0023	0,0007
0702	0,0035	0,0057	1,6286	0,0064	0,0094	0,0039	2,2688	0,0087	0,0038
1002	0,0025	0,0038	1,5200	0,0047	0,0074	0,0031	2,5716	0,0057	0,0022
1102	0,0012	0,0018	1,5000	0,0022	0,0033	0,0015	2,9700	0,0032	0,0011

Grey boxes denote lesion group

(*) denotes an AUC decrease after the 'lesion' compared to before

Supplementary Table 3

Suppl. Table 3. AUC values normalized to the indifferent baseline.

		Background: 1,0-4,8Hz				Theta Low: 4,8-8,18Hz			
		Before	/Indif	After	/Indif	Before	/Indif	After	/Indif
Indifferent		0,0109				0,0052			
2112	5	0,0136	1,2477	0,0154	1,4128	0,0081	1,5577	0,0111	2,1346
	6	0,0110	1,0092	0,0131	1,2018	0,0065	1,2500	0,0097	1,8654
	7	0,0139	1,2752	0,0110	1,0092	0,0056	1,0769	0,0073	1,4038
	8	0,0103	0,9450	0,0068	0,6239	0,0060	1,1538	0,0061	1,1731
	9	0,0089	0,8165	0,0074	0,6789	0,0065	1,2500	0,0055	1,0577
	10	0,0070	0,6422	0,0070	0,6422	0,0058	1,1154	0,0054	1,0385
Base		0,0150	1,3761	0,0126	1,1560	0,0073	1,4038	0,0113	2,1731
Indifferent		0,0043				0,0021			
0601	5	0,0032	0,7442	0,0066	1,5349	0,0026	1,2381	0,0034	1,6190
	6	0,0052	1,2093	0,0060	1,3953	0,0034	1,6190	0,0034	1,6190
	7	0,0050	1,1628	0,0051	1,1860	0,0031	1,4762	0,0038	1,8095
	8	0,0052	1,2093	0,0060	1,3953	0,0031	1,4762	0,0036	1,7143
	9	0,0046	1,0698	0,0044	1,0233	0,0026	1,2381	0,0034	1,6190
	10	0,0173	4,0233	0,0049	1,1395	0,0122	5,8095	0,0034	1,6190
Base		0,0076	1,7674	0,0074	1,7209	0,0036	1,7143	0,0036	1,7143
Indifferent		0,0008				0,0018			
2701	5	0,0052	6,5000	0,0047	5,8750	0,0037	2,0556	0,0044	2,4444
	6	0,0033	4,1250	0,0063	7,8750	0,0028	1,5556	0,0052	2,8889
	7	0,0059	7,3750	0,0056	7,0000	0,0034	1,8889	0,0052	2,8889
	8	0,0059	7,3750	0,0051	6,3750	0,0027	1,5000	0,0038	2,1111
	9	0,0064	8,0000	0,0033	4,1250	0,0044	2,4444	0,0028	1,5556
	10	0,0060	7,5000	0,0064	8,0000	0,0048	2,6667	0,0057	3,1667
Base		0,0049	6,1250	0,0062	7,7500	0,0034	1,8889	0,0025	1,3889
Indifferent		0,0047				0,0028			
0102	5	0,0126	2,6809	0,0128	2,7234	0,0086	3,0714	0,0077	2,7500
	6	0,0104	2,2128	0,0131	2,7872	0,0072	2,5714	0,0088	3,1429
	7	0,0088	1,8723	0,0125	2,6596	0,0061	2,1786	0,0072	2,5714
	8	0,0081	1,7234	0,0090	1,9149	0,0066	2,3571	0,0047	1,6786
	9	0,0098	2,0851	0,0048	1,0213	0,0079	2,8214	0,0030	1,0714
	10	0,0075	1,5957	0,0086	1,8298	0,0050	1,7857	0,0038	1,3571
Base		0,0277	5,8936	0,0291	6,1915	0,0108	3,8571	0,0109	3,8929
Indifferent		0,0027				0,0022			
0902	5	0,0052	1,9259	0,0055	2,0370	0,0028	1,2727	0,0031	1,4091
	6	0,0064	2,3704	0,0045	1,6667	0,0026	1,1818	0,0027	1,2273
	7	0,0057	2,1111	0,0047	1,7407	0,0029	1,3182	0,0033	1,5000
	8	0,0056	2,0741	0,0052	1,9259	0,0035	1,5909	0,0030	1,3636
	9	0,0056	2,0741	0,0055	2,0370	0,0028	1,2727	0,0029	1,3182

	10	0,0050	1,8519	0,0060	2,2222	0,0027	1,2273	0,0023	1,0455
Base		0,0051	1,8889	0,0059	2,1852	0,0030	1,3636	0,0033	1,5000
Indifferent		**0,0011**				**0,0011**			
1502	5	0,0044	4,0000	0,0059	5,3636	0,0026	2,3636	0,0024	2,1818
	6	0,0049	4,4545	0,0052	4,7273	0,0021	1,9091	0,0028	2,5455
	7	0,0047	4,2727	0,0077	7,0000	0,0023	2,0909	0,0019	1,7273
	8	0,0051	4,6364	0,0052	4,7273	0,0023	2,0909	0,0020	1,8182
	9	0,0053	4,8182	0,0068	6,1818	0,0028	2,5455	0,0027	2,4545
	10	0,0042	3,8182	0,0060	5,4545	0,0021	1,9091	0,0024	2,1818
Base		0,0060	5,4545	0,0057	5,1818	0,0026	2,3636	0,0025	2,2727
Indifferent		**0,0075**				**0,0033**			
2212	5	0,0082	1,0933	0,0086	1,1467	0,0046	1,3939	0,0050	1,5152
	6	0,0081	1,0800	0,0103	1,3733	0,0055	1,6667	0,0045	1,3636
	7	0,0103	1,3733	0,0067	0,8933	0,0055	1,6667	0,0061	1,8485
	8	0,0099	1,3200	0,0088	1,1733	0,0052	1,5758	0,0042	1,2727
	9	0,0093	1,2400	0,0089	1,1867	0,0049	1,4848	0,0057	1,7273
	10	0,0066	0,8800	0,0085	1,1333	0,0035	1,0606	0,0056	1,6970
Base		0,0087	1,1600	0,0073	0,9733	0,0050	1,5152	0,0050	1,5152
Indifferent		**0,0014**				**0,0022**			
2601	5	0,0079	5,6429	0,0130	9,2857	0,0054	2,4545	0,0026	1,1818
	6	0,0085	6,0714	0,0142	10,1429	0,0043	1,9545	0,0048	2,1818
	7	0,0101	7,2143	0,0206	14,7143	0,0044	2,0000	0,0047	2,1364
	8	0,0192	13,7143	0,0320	22,8571	0,0048	2,1818	0,0071	3,2273
	9	0,0144	10,2857	0,0253	18,0714	0,0048	2,1818	0,0050	2,2727
	10	0,0107	7,6429	0,0320	22,8571	0,0039	1,7727	0,0068	3,0909
Base		0,0078	5,5714	0,0150	10,7143	0,0065	2,9545	0,0082	3,7273
Indifferent		**0,0017**				**0,0016**			
0302	5	0,0030	1,7647	0,0040	2,3529	0,0017	1,0625	0,0021	1,3125
	6	0,0032	1,8824	0,0040	2,3529	0,0017	1,0625	0,0025	1,5625
	7	0,0023	1,3529	0,0044	2,5882	0,0012	0,7500	0,0022	1,3750
	8	0,0016	0,9412	0,0047	2,7647	0,0011	0,6875	0,0017	1,0625
	9	0,0027	1,5882	0,0049	2,8824	0,0015	0,9375	0,0026	1,6250
	10	0,0026	1,5294	0,0032	1,8824	0,0015	0,9375	0,0022	1,3750
Base		0,0016	0,9412	0,0051	3,0000	0,0012	0,7500	0,0023	1,4375
Indifferent		**0,0069**				**0,0056**			
0702	5	0,0082	1,1884	0,0083	1,2029	0,0065	1,1607	0,0059	1,0536
	6	0,0080	1,1594	0,0098	1,4203	0,0059	1,0536	0,0084	1,5000
	7	0,0082	1,1884	0,0111	1,6087	0,0053	0,9464	0,0067	1,1964
	8	0,0097	1,4058	0,0074	1,0725	0,0060	1,0714	0,0043	0,7679
	9	0,0074	1,0725	0,0080	1,1594	0,0047	0,8393	0,0057	1,0179
	10	0,0090	1,3043	0,0073	1,0580	0,0050	0,8929	0,0058	1,0357
Base		0,0093	1,3478	0,0170	2,4638	0,0049	0,8750	0,0065	1,1607
Indifferent		**0,0018**				**0,0012**			

1002	5	0,0072	4,0000	0,0071	3,9444	0,0024	2,0000	0,0044	3,6667
	6	0,0074	4,1111	0,0074	4,1111	0,0038	3,1667	0,0041	3,4167
	7	0,0071	3,9444	0,0082	4,5556	0,0031	2,5833	0,0040	3,3333
	8	0,0072	4,0000	0,0049	2,7222	0,0037	3,0833	0,0035	2,9167
	9	0,0076	4,2222	0,0091	5,0556	0,0037	3,0833	0,0045	3,7500
	10	0,0074	4,1111	0,0073	4,0556	0,0035	2,9167	0,0041	3,4167
Base		0,0056	3,1111	0,0085	4,7222	0,0031	2,5833	0,0040	3,3333
Indifferent		**0,0019**				**0,001**			
1102	5	0,0057	3,0000	0,0059	3,1053	0,0022	2,2000	0,0028	2,8000
	6	0,0048	2,5263	0,0075	3,9474	0,0021	2,1000	0,0032	3,2000
	7	0,0038	2,0000	0,0073	3,8421	0,0024	2,4000	0,0031	3,1000
	8	0,0045	2,3684	0,0057	3,0000	0,0022	2,2000	0,0043	4,3000
	9	0,0035	1,8421	0,0070	3,6842	0,0020	2,0000	0,0021	2,1000
	10	0,0039	2,0526	0,0046	2,4211	0,0032	3,2000	0,0026	2,6000
Base		0,0036	1,8947	0,0081	4,2632	0,0025	2,5000	0,0038	3,8000

Grey boxes denote lesion group

Suppl. Table 3. AUC values normalized to the indifferent baseline (continued).

		Theta Driven: 8,19-11,82Hz				**Beta Low: 11,83-17,99Hz**			
		Before	**/Indif**	**After**	**/Indif**	**Before**	**/Indif**	**After**	**/Indif**
Indifferent		**0,0053**				**0,0087**			
2112	5	0,0138	2,6038	0,0257	4,8491	0,0100	1,1494	0,0221	2,5402
	6	0,0144	2,7170	0,0256	4,8302	0,0101	1,1609	0,0134	1,5402
	7	0,0193	3,6415	0,0190	3,5849	0,0112	1,2874	0,0095	1,0920
	8	0,0202	3,8113	0,0164	3,0943	0,0090	1,0345	0,0090	1,0345
	9	0,0160	3,0189	0,0188	3,5472	0,0085	0,9770	0,0096	1,1034
	10	0,0160	3,0189	0,0164	3,0943	0,0103	1,1839	0,0088	1,0115
Base		0,0062	1,1698	0,0131	2,4717	0,0122	1,4023	0,0210	2,4138
Indifferent		**0,0013**				**0,0019**			
0601	5	0,0051	3,9231	0,0091	7,0000	0,0032	1,6842	0,0058	3,0526
	6	0,0071	5,4615	0,0098	7,5385	0,0043	2,2632	0,0055	2,8947
	7	0,0073	5,6154	0,0091	7,0000	0,0041	2,1579	0,0081	4,2632
	8	0,0096	7,3846	0,0104	8,0000	0,0062	3,2632	0,0055	2,8947
	9	0,0082	6,3077	0,0094	7,2308	0,0071	3,7368	0,0049	2,5789
	10	0,0140	10,7692	0,0085	6,5385	0,0142	7,4737	0,0073	3,8421
Base		0,0023	1,7692	0,0038	2,9231	0,0028	1,4737	0,0050	2,6316
Indifferent		**0,0007**				**0,0011**			
2701	5	0,0066	9,4286	0,0066	9,4286	0,0040	3,6364	0,0073	6,6364
	6	0,0038	5,4286	0,0079	11,2857	0,0025	2,2727	0,0069	6,2727
	7	0,0042	6,0000	0,0070	10,0000	0,0035	3,1818	0,0060	5,4545
	8	0,0061	8,7143	0,0061	8,7143	0,0039	3,5455	0,0039	3,5455
	9	0,0092	13,1429	0,0046	6,5714	0,0064	5,8182	0,0032	2,9091
	10	0,0097	13,8571	0,0071	10,1429	0,0065	5,9091	0,0066	6,0000

Base		0,0025	3,5714	0,0035	5,0000	0,0046	4,1818	0,0066	6,0000
Indifferent		**0,002**				**0,003**			
0102	5	0,0151	7,5500	0,0086	4,3000	0,0163	5,4333	0,0111	3,7000
	6	0,0090	4,5000	0,0191	9,5500	0,0107	3,5667	0,0211	7,0333
	7	0,0107	5,3500	0,0150	7,5000	0,0104	3,4667	0,0100	3,3333
	8	0,0107	5,3500	0,0119	5,9500	0,0098	3,2667	0,0072	2,4000
	9	0,0153	7,6500	0,0052	2,6000	0,0109	3,6333	0,0052	1,7333
	10	0,0136	6,8000	0,0122	6,1000	0,0082	2,7333	0,0080	2,6667
Base		0,0104	5,2000	0,0107	5,3500	0,0157	5,2333	0,0144	4,8000
Indifferent		**0,002**				**0,0033**			
0902	5	0,0034	1,7000	0,0029	1,4500	0,0057	1,7273	0,0048	1,4545
	6	0,0031	1,5500	0,0022	1,1000	0,0050	1,5152	0,0031	0,9394
	7	0,0028	1,4000	0,0026	1,3000	0,0041	1,2424	0,0046	1,3939
	8	0,0037	1,8500	0,0026	1,3000	0,0048	1,4545	0,0050	1,5152
	9	0,0029	1,4500	0,0030	1,5000	0,0053	1,6061	0,0047	1,4242
	10	0,0030	1,5000	0,0027	1,3500	0,0050	1,5152	0,0048	1,4545
Base		0,0038	1,9000	0,0028	1,4000	0,0065	1,9697	0,0051	1,5455
Indifferent		**0,0005**				**0,0008**			
1502	5	0,0025	5,0000	0,0025	5,0000	0,0049	6,1250	0,0054	6,7500
	6	0,0023	4,6000	0,0029	5,8000	0,0030	3,7500	0,0042	5,2500
	7	0,0023	4,6000	0,0024	4,8000	0,0046	5,7500	0,0052	6,5000
	8	0,0020	4,0000	0,0036	7,2000	0,0031	3,8750	0,0045	5,6250
	9	0,0032	6,4000	0,0040	8,0000	0,0042	5,2500	0,0052	6,5000
	10	0,0037	7,4000	0,0031	6,2000	0,0032	4,0000	0,0053	6,6250
Base		0,0024	4,8000	0,0025	5,0000	0,0035	4,3750	0,0037	4,6250
Indifferent		**0,0035**				**0,0065**			
2212	5	0,0099	2,8286	0,0090	2,5714	0,0062	0,9538	0,0063	0,9692
	6	0,0097	2,7714	0,0092	2,6286	0,0067	1,0308	0,0095	1,4615
	7	0,0117	3,3429	0,0140	4,0000	0,0062	0,9538	0,0111	1,7077
	8	0,0095	2,7143	0,0080	2,2857	0,0053	0,8154	0,0058	0,8923
	9	0,0098	2,8000	0,0096	2,7429	0,0070	1,0769	0,0080	1,2308
	10	0,0082	2,3429	0,0083	2,3714	0,0041	0,6308	0,0078	1,2000
Base		0,0055	1,5714	0,0048	1,3714	0,0105	1,6154	0,0083	1,2769
Indifferent		**0,001**				**0,0013**			
2601	5	0,0060	6,0000	0,0051	5,1000	0,0090	6,9231	0,0044	3,3846
	6	0,0049	4,9000	0,0054	5,4000	0,0074	5,6923	0,0077	5,9231
	7	0,0070	7,0000	0,0066	6,6000	0,0084	6,4615	0,0089	6,8462
	8	0,0053	5,3000	0,0067	6,7000	0,0076	5,8462	0,0092	7,0769
	9	0,0076	7,6000	0,0064	6,4000	0,0077	5,9231	0,0085	6,5385
	10	0,0079	7,9000	0,0083	8,3000	0,0065	5,0000	0,0093	7,1538
Base		0,0035	3,5000	0,0049	4,9000	0,0072	5,5385	0,0079	6,0769
Indifferent		**0,0011**				**0,0012**			
0302	5	0,0013	1,1818	0,0023	2,0909	0,0020	1,6667	0,0032	2,6667

	6	0,0013	1,1818	0,0025	2,2727	0,0021	1,7500	0,0031	2,5833
	7	0,0013	1,1818	0,0021	1,9091	0,0020	1,6667	0,0036	3,0000
	8	0,0015	1,3636	0,0025	2,2727	0,0022	1,8333	0,0043	3,5833
	9	0,0024	2,1818	0,0029	2,6364	0,0028	2,3333	0,0037	3,0833
	10	0,0021	1,9091	0,0033	3,0000	0,0026	2,1667	0,0042	3,5000
Base		0,0013	1,1818	0,0018	1,6364	0,0021	1,7500	0,0038	3,1667
Indifferent		**0,0054**				**0,0072**			
0702	5	0,0093	1,7222	0,0122	2,2593	0,0079	1,0972	0,0094	1,3056
	6	0,0084	1,5556	0,0137	2,5370	0,0090	1,2500	0,0092	1,2778
	7	0,0097	1,7963	0,0117	2,1667	0,0079	1,0972	0,0100	1,3889
	8	0,0100	1,8519	0,0078	1,4444	0,0100	1,3889	0,0051	0,7083
	9	0,0115	2,1296	0,0131	2,4259	0,0072	1,0000	0,0068	0,9444
	10	0,0120	2,2222	0,0155	2,8704	0,0089	1,2361	0,0086	1,1944
Base		**0,0052**	0,9630	**0,0049**	0,9074	**0,0064**	0,8889	**0,0094**	1,3056
Indifferent		**0,0011**				**0,0016**			
1002	5	0,0048	4,3636	0,0053	4,8182	0,0068	4,2500	0,0070	4,3750
	6	0,0035	3,1818	0,0038	3,4545	0,0060	3,7500	0,0081	5,0625
	7	0,0035	3,1818	0,0048	4,3636	0,0052	3,2500	0,0067	4,1875
	8	0,0037	3,3636	0,0037	3,3636	0,0070	4,3750	0,0065	4,0625
	9	0,0042	3,8182	0,0037	3,3636	0,0062	3,8750	0,0063	3,9375
	10	0,0043	3,9091	0,0041	3,7273	0,0066	4,1250	0,0085	5,3125
Base		0,0032	2,9091	0,0041	3,7273	0,0047	2,9375	0,0074	4,6250
Indifferent		**0,001**				**0,0014**			
1102	5	0,0045	4,5000	0,0050	5,0000	0,0024	1,7143	0,0032	2,2857
	6	0,0043	4,3000	0,0067	6,7000	0,0026	1,8571	0,0041	2,9286
	7	0,0040	4,0000	0,0050	5,0000	0,0025	1,7857	0,0029	2,0714
	8	0,0033	3,3000	0,0058	5,8000	0,0024	1,7143	0,0045	3,2143
	9	0,0033	3,3000	0,0049	4,9000	0,0022	1,5714	0,0025	1,7857
	10	0,0040	4,0000	0,0052	5,2000	0,0033	2,3571	0,0044	3,1429
Base		0,0020	2,0000	0,0029	2,9000	0,0022	1,5714	0,0033	2,3571

Grey boxes denote lesion group

Suppl. Table 3. AUC values normalized to the indifferent baseline.

		Beta Driven: 18-22Hz			
		Before	/Indif	After	/Indif
Indifferent		**0,0033**			
2112	5	0,0084	2,5455	0,0138	4,1818
	6	0,0100	0,3030	0,0108	3,2727
	7	0,0125	3,7879	0,0119	3,6061
	8	0,0117	3,5455	0,0135	4,0909
	9	0,0128	3,8788	0,0119	3,6061
	10	0,0132	4,0000	0,0121	3,6667
Base		0,0048	1,4545	0,0087	2,6364

Indifferent		0,001			
0601	5	0,0020	2,0000	0,0043	4,3000
	6	0,0023	2,3000	0,0048	4,8000
	7	0,0032	3,2000	0,0047	4,7000
	8	0,0072	7,2000	0,0051	5,1000
	9	0,0042	4,2000	0,0040	4,0000
	10	0,0084	8,4000	0,0059	5,9000
Base		0,0014	1,4000	0,0025	2,5000
Indifferent		**0,0007**			
2701	5	0,0029	4,1429	0,0051	7,2857
	6	0,0018	2,5714	0,0057	8,1429
	7	0,0025	3,5714	0,0045	6,4286
	8	0,0030	4,2857	0,0033	4,7143
	9	0,0047	6,7143	0,0033	4,7143
	10	0,0046	6,5714	0,0052	7,4286
Base		0,0025	3,5714	0,0038	5,4286
Indifferent		**0,0013**			
0102	5	0,0118	9,0769	0,0085	6,5385
	6	0,0102	7,8462	0,0126	9,6923
	7	0,0118	9,0769	0,0110	8,4615
	8	0,0126	9,6923	0,0101	7,7692
	9	0,0152	11,6923	0,0095	7,3077
	10	0,0148	11,3846	0,0124	9,5385
Base		0,0085	6,5385	0,009	6,9231
Indifferent		**0,0014**			
0902	5	0,0028	2,0000	0,0024	1,7143
	6	0,0025	1,7857	0,0018	1,2857
	7	0,0032	2,2857	0,0023	1,6429
	8	0,0030	2,1429	0,0022	1,5714
	9	0,0028	2,0000	0,0024	1,7143
	10	0,0031	2,2143	0,0026	1,8571
Base		0,0026	1,8571	0,0025	1,7857
Indifferent		**0,0003**			
1502	5	0,0023	7,6667	0,0030	10,0000
	6	0,0015	5,0000	0,0026	8,6667
	7	0,0022	7,3333	0,0036	12,0000
	8	0,0015	5,0000	0,0025	8,3333
	9	0,0018	6,0000	0,0028	9,3333
	10	0,0024	8,0000	0,0025	8,3333
Base		0,0018	6,0000	0,0020	6,6667
Indifferent		**0,003**			
2212	5	0,0078	2,6000	0,0046	1,5333
	6	0,0075	2,5000	0,0048	1,6000

	7	0,0078	2,6000	0,0051	1,7000
	8	0,0085	2,8333	0,0057	1,9000
	9	0,0098	3,2667	0,0074	2,4667
	10	0,0083	2,7667	0,0072	2,4000
Base		0,0065	2,1667	0,0050	1,6667
Indifferent		**0,0006**			
2601	5	0,0057	9,5000	0,0032	5,3333
	6	0,0053	8,8333	0,0042	7,0000
	7	0,0041	6,8333	0,0050	8,3333
	8	0,0045	7,5000	0,0047	7,8333
	9	0,0051	8,5000	0,0042	7,0000
	10	0,0037	6,1667	0,0049	8,1667
Base		0,0039	6,5000	0,0032	5,3333
Indifferent		**0,0007**			
0302	5	0,0011	1,5714	0,0022	3,1429
	6	0,0011	1,5714	0,0028	4,0000
	7	0,0013	1,8571	0,0031	4,4286
	8	0,0014	2,0000	0,0030	4,2857
	9	0,0016	2,2857	0,0028	4,0000
	10	0,0017	2,4286	0,0042	6,0000
Base		0,0010	1,4286	0,0028	4,0000
Indifferent		**0,0038**			
0702	5	0,0073	1,9211	0,0111	2,9211
	6	0,0103	2,7105	0,0079	2,0789
	7	0,0073	1,9211	0,0102	2,6842
	8	0,0092	2,4211	0,0066	1,7368
	9	0,0093	2,4474	0,0140	3,6842
	10	0,0102	2,6842	0,0135	3,5526
Base		0,0035	0,9211	0,0057	1,5000
Indifferent		**0,001**			
1002	5	0,0037	3,7000	0,0035	3,5000
	6	0,0032	3,2000	0,0043	4,3000
	7	0,0032	3,2000	0,0036	3,6000
	8	0,0031	3,1000	0,0031	3,1000
	9	0,0033	3,3000	0,0038	3,8000
	10	0,0033	3,3000	0,0038	3,8000
Base		0,0025	2,5000	0,0038	3,8000
Indifferent		**0,0005**			
1102	5	0,0016	3,2000	0,0016	3,2000
	6	0,0014	2,8000	0,0025	5,0000
	7	0,0013	2,6000	0,0017	3,4000
	8	0,0010	2,0000	0,0033	6,6000
	9	0,0011	2,2000	0,0023	4,6000

	10	0,0021	4,2000	0,0024	4,8000
Base		0,0012	2,4000	0,0018	3,6000

Grey boxes denote lesion group

Supplementary Table 4

Suppl Table 4: Literature references for theta-frequency.

Frequency (Hz)	Lower Bond	Upper Bond	References (by first author)
3-12	3	12	Bland (3,6,39,66,67,*Hippocampus 2003;13(1):38-47*, *Synapse 2007;61(3):185-197*); Colom (49,55,73,82,99); Oddie (46,68,69,95); Gallagher (*Prog Neurobiol 1995;45:373-395*); Orzel-Gryglewski (*Brain Res Bull 2006;68(5):295-309*); Hyman (*J Neurosci 2003;23(37):11725-11731*); Natsume (*Hippocampus 1999;9:500-509*); Scarlett (41)
5-10	5	10	Buzsaki (62); Donovick (15); Winson (18); Gengler (*Behav Brain Res 2005;164(1):73-82*); Jensen (*Trends Cogn Sci 2005;9(12):551-553*); Mizesuki (*Neuron 2009;64(Oct 29): 267-280*); Gray (29)
6-12	6	12	Kramis (27,28); Vanderwolf (9); Leung (*Neurosci Biobehav R 1998;22(2)275-290*)
5-12	5	12	Zhou (*Hippocampus 1999;9:220-234*); Denham (*Hippocampus 2000;10:698-716*) Vertes (56,79)
5-11	5	11	Gray (16)
4-10	4	10	Buzsaki (32, *Cereb Cortex 1996 Mar-Apr;6(2):81-92*); Hangya (51); Yoder (45); Stewart (11)
4-12	4	12	Kramis (4); Kroplewski (); Lu (*Neuroscience 2011;17(177):1-11*); Manseau (59); O'Keefe (98); Sainsbury (10); McNaughton (*Brain Res 1980;200:259-269*); Williams (80); Partlo (20)
6-10	6	10	Ball (30); Whishaw (101); Dragoi (*J Neurosci 1999 Jul 15;19(14):6191-6199*); Drewett (*Neuroscience 1977;2:1033-1041*); Gray (40); James (26); McNaughton (*Neuroscience 1977;2: 1019-1027*); Valero (*Neuroscience 1977;2(6): 1029-1032*)
6-14	6	14	Rawlins (17)
4-14	4	14	Heynen (*NeuroReport 1991;2: 401-404*)
3,5-13	3,5	13	Wetzel (42)
Average	***4,68***	***11,82***	